Spring 5-31-2016

Continuum mechanical analysis of space and time dependent deformation pattern of brain with blunt injury

Chen Miao
New Jersey Institute of Technology

Copyright Warning & Restrictions

The copyright law of the United States (Title 17, United States Code) governs the making of photocopies or other reproductions of copyrighted material.

Under certain conditions specified in the law, libraries and archives are authorized to furnish a photocopy or other reproduction. One of these specified conditions is that the photocopy or reproduction is not to be "used for any purpose other than private study, scholarship, or research." If a, user makes a request for, or later uses, a photocopy or reproduction for purposes in excess of "fair use" that user may be liable for copyright infringement,

This institution reserves the right to refuse to accept a copying order if, in its judgment, fulfillment of the order would involve violation of copyright law.

Please Note: The author retains the copyright while the New Jersey Institute of Technology reserves the right to distribute this thesis or dissertation

Printing note: If you do not wish to print this page, then select "Pages from: first page # to: last page #" on the print dialog screen

ABSTRCT

CONTINUUM MECHANICAL ANALYSIS OF SPACE AND TIME DEPENDENT DEFORMATION PATTERN OF BRAIN WITH BLUNT INJURY

by
Chen Miao

Deformation of human brain due to acceleration impact has been widely accepted as the direct connection to the Trauma Brain Injury (TBI). However, the limitation of obtaining deformation data of TBI is a major obstacle to understanding TBI mechanism. This experiment mainly focuses on developing a method to measure deformation pattern of brain with blunt injury. First of all, displacement data of markers on sagittal plane of an injury head model was collected using 3D reconstruction software after an impact test. Second, the displacement data was used to calculate 2D Lagrangian strain tensor and the principal strain. The temporal and spatial results of principal strain under different variables including impact velocity (5 mile/hour, 3 mile/ hour), impact location (crown head, front head) and concentration of gel used to build the brain model (10%, 20%) were compared. The results shown larger strain values within the variables of higher impact velocity, crown head impact location and 10% gel. The spatial location results shown clearly the difference in terms of deformation pattern of different impact locations.

CONTINUUM MECHANICAL ANALYSIS OF SPACE AND TIME DEPENDENT DEFORMATION PATTERN OF BRAIN WITH BLUNT INJURY

by
Chen Miao

A Thesis
Submitted to the Faculty of
New Jersey Institute of Technology
in Partial Fulfillment of the Requirements for the Degree of
Master of Science in Biomedical Engineering

Department of Biomedical Engineeing

May 2016

APPROVAL PAGE

CONTINUUM MECHANICAL ANALYSIS OF SPACE AND TIME DEPENDENT DEFORMATION PATTERN OF BRAIN WITH BLUNT INJURY

Chen Miao

Dr. Bryan J. Pfister, Thesis Advisor — Date
Associate Professor of Biomedical Engineering, NJIT

Dr. Namas Chandra, Committee Member — Date
Professor of Biomedical Engineering, NJIT

Dr. Max Roman, Committee Member — Date
Assistant Research Professor of Biomedical Engineering, NJIT

BIOGRAPHICAL SKETCH

Author: Chen Miao

Degree: Master of Science

Date: May, 2016

Undergraduate and Graduate Education:

- Master of Science in Biomedical Engineering,
  New Jersey Institute of Technology, Newark, NJ, 2016

- Bachelor of Science in Biological Science,
  Zhejiang Chinese Medical University, Hangzhou, P. R. China, 2014

Major: Biomedical Engineering

The thesis dedicated to
The two parts of my life: My parents,
Without you, my life will fall down.

Mother, you gave me birth and tell me to keep smile to both darkness and sunshine, I can’t be much more grateful for your love.

Father, you are the one who taught me how to be thoughtful in front of difficulties, I will always keep in mind what you have told me.

ACKNOWLEDGEMENT

First of all, I want to express my appreciation to my thesis advisor, friendly and patient Dr. Bryan J. Pfister, from whom I obtained so much valuable knowledge from the field of Biomechanics. Second，I really want to thank the committee members of my thesis, Dr. Namas Chandra, who has gave me some guide for Continuum Mechanic field, and Dr. Max Roman, who brought my into the biomechanics world. And also I really learned a lot especially the programming of Matlab from my dear school fellow, Mr. Swenson Brian, I can definitely not finish my thesis perfectly without your great help.

TABLE OF CONTENTS

Chapter		Page
1	INTRODUCTION…….....	1
	1.1 Briefly Introduction of TBI…….....	1
	1.2 Mechanics of TBI…….....	2
	1.3 Background of Deformation Measurement in TBI Research…….	3
	1.4 Continnum Analysis in Deformation Measurement……	6
	1.5 Conclusion……	12
2	OBJECTIVE…….....	14
3	METHOD……..	15
	3.1 Design of Head Model……...	15
	3.1.1 Casting Design of Head Model……..	16
	3.1.2 Assembly of the Dead Model and Neck……	18
	3.2 Drop Impact Tower Test and High Speed Video Imaging System……	19
	3.3 3D Kinematic Reconstruction and Data Acquisition……	25
	3.4 Calculation of Strain Tensor and Principal Strain…….	30
	3.5 Presenting Results with Matlab and Minitab…….	34
4	RESULTS AND DISCUSSION…….	35
	4.1 Comparison of Results with Different Impact Velocities…….	35
	4.2 Comparison of Results with Different Impact Locations……..	42
	4.3 Comparison of Results with Different Gel concentrations……	48
5	CONCLUSION AND FUTURE WORK……	53
	REFERENCES…….	55

LIST OF FIGURES

Figure		Page
1.1	TBI - Worldwide Totals Q1-Q3 2014.....	2
1.2	Displacement of Continuum Body……...	8
1.3	Snapshots of Deformed and Undeformed States of Silicon Substrates…….	12
3.1	The Full Structure of the Head Model.....	18
3.2	The Neck of Hybrid III Anthropomorphic Test Device……..……	19
3.3	The Epoxy Layer…….....……	19
3.4	The High Speed 3D video Imaging System…….	20
3.5	The Basic Structure of the Impact Machine……...……..	21
3.6	The Impactor with Head Shape……..……..	23
3.7	Shelf with 45 Degree Angle……..……...	25
3.8	Comparison of Original Video Picture and Filtered Video Picture.....	27
3.9	Calibration Process Using ProAnalyst……...……..	28
3.10	The 2D Tracking Process Using ProAnalyst……..……..	29
3.11	The Final Step of Using ProAnalyst……..……..	30
3.12	Numbering of the Markers and the Squares…….	32
3.13	Two Vectors used for Creating the Deformation Gradient Tensor…..	33
3.14	Numbers of 72 Squares Indicating the Specific Spatial Socation on the Surface of the Sagittal Plane……..	34
4.1	Definition of the Rise Time……..……	36
4.2	Strain Value Comparison Between Different Impact Heights……..	37

LIST OF FIGURES
(Continued)

Figure		Page
4.3	Rise Time Comparison Between Different Impact Velocities……..	38
4.4	Four Quadrants used for Describing the Specific Location of Maximum Strain and Deformation Pattern……..	39
4.5	Spatial Location Comparison between Different Impact Velocities…	40
4.6	Comparison of Contour Plotting 72 Squares…….....	41
4.7	Different Impact Locations Including Crown Head and Fore Head…	42
4.8	Strain Value Comparison between Different Impact Locations……...	44
4.9	Rise Time Comparison between Different Impact Locations……..	44
4.10	Spatial Location Comparison between Different Impact Locations…	46
4.11	Comparison of Contour Plotting All 72 squares Between Different Impact Locations……..	47
4.12	Strain Value Comparison between Different Gel Concentrations……	48
4.13	Rise Time Comparison between Different Gel Concentrations……...	49
4.14	Spatial Location Comparison between Different Gel Concentrations.	51
4.15	Comparison of Contour Plotting All 72 Squares between Different Gel Concentrations……...	52

LIST OF TABLES

Table		Page
3.1	Information for Materials used for Creating Head Models…….	16
3.2	Different Impact Heights with Different Impact Velocities…….	22
3.3	Summary of 3 Variables and Hit Times used in the Impact Test…….	24
4.1	Strain Value and Spatial Location Data of the 20 Percent Gel Model with Crown Head Impact Position and 3 Mph Impact Velocity……..	36
4.2	Strain Value and Spatial Location Data of 20 Percent Gel Model with Crown Head Impact Position and 5 Mph Impact Velocity……..	36
4.3	Strain Value and Spatial Location Data of 20 Percent Gel Model with Front Head Impact Position and 3 Mph Impact Velocity……	42
4.4	Strain Value and Spatial Location Data of 10 Percent Gel Model with Front Head Impact Position and 3 Mph Impact Velocity……	48
4.5	Mean Distance Between Two Spatial Locations of Maximum Strain Value of Different Concentration of Gels……	50

CHAPTER 1

INTRODUCTION

1.1 Introduction of TBI

Traumatic Brain Injury (TBI) has been a serious problem in public health field throughout the world especially in recent several years: In United States, according to the data base of Centers for Disease Control and Prevention (CDC), the total rates of TBI including hospitalizations, Emergency Department (EM) visits and Deaths had increased from 521.0 per 100,000 in 2001 to 823.7 per 100,000 in 2010[1]. There are nearly 8 billion dollars cost related to the treatment and other medical related expense covering the TBI problem and more than 1 million new relevant patients every year [2]. In addition, TBI is regarded as a principle reason for the disability and death among adults ranged from 15 to 45[3]. TBI can be classified as mild when the time of loss consciousness is less than 30 minutes, which is the most prevalent TBI and can cause memory loss (Figure 1.1), visual disturbance, poor concentration and lead further neurological symptoms [4].

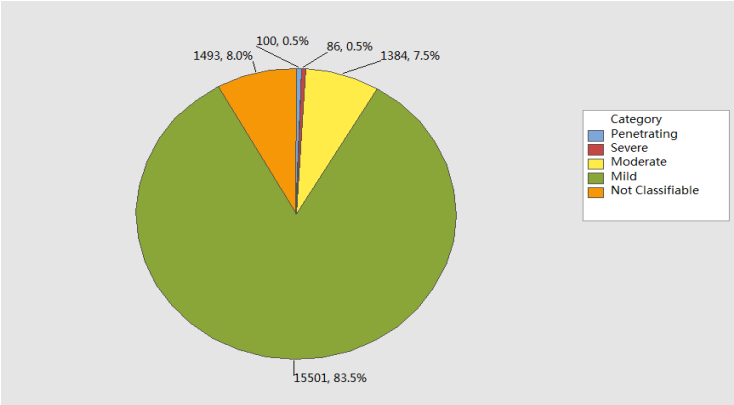

Figure 1.1 Numbers and percentage of different kinds of TBI worldwide during first three quarters in 2014, the total number of all severities is 18564, which comes from the database of U.S. Department of Defense.
Source: http://archive.defense.gov/home/features/2015/0315_tbi/(access on March 16, 2016)

1.2 Mechanics of TBI

Usually, TBI is caused by an external force to the brain that causes traumatic injury, among which car accidents, firearms and falls are the three major causes[5]. It is widely accepted that the soft tissue of brain will deform inside the skull due to acceleration of the whole head, such as the blunt impact during a crime scene where the criminal hits a victim's head; and deceleration, such as the movement of two football players colliding with each other from opposite directions with high speed. In other words, the brain tissue will be stretched or compressed during the back and forth movement and produce deformation due to diffuse axonal shearing. The deformation can lead to the damage of axons and neurons of the brain [6]. Accordingly, the overall hypothesis of this work is that the causal mechanism of TBI is strongly related to the spatial and temporal deformation pattern of the brain tissue.

1.3 Background of Deformation Measurement in TBI Research

The exact details of the deformation of brain from blunt injury to the head are still not very clear. The research of Robert H. Pudenz in 1946[7] developed a surgical experiment during which part of a monkey skull was replaced by a transparent lucite calvarium in order to investigate the physical changes in the brain from cranial trauma, this was one of the early research published to study the physical mechanics of TBI using animal experiment, however, the limitation of the experiment is obvious, nothing that happened inside of the brain can be observed even if the surface deformation of brain can be observed. Recently, some new technologies have been used for deformation analysis in terms of animal experiment, such as Erin E. Black [8] and his team, who used Magnetic Resonance Image (MRI) technique to study the spatial and temporal deformation pattern of brain during skull acceleration with perinatal rats, through which the internal deformation pattern can be visualized better. This point can also be demonstrated by the research of Wei Liu and his team [9], during which a Harmonic Phase (HARP) Analysis was use to quantify the lagrangian strain field in rat hearts during myocardial wall motion with MR images. However, the limitations of these studies still exist, the difference in the size and structure of the brain between human and animal simply cannot be ignored. Additionally, due to restrictions of the experimental techniques, normal injury conditions were not achieved.

With the development of technologies, researchers also developed computational simulations to mimic injury head model under concussion conditions in order to investigating the biomechanics, such as the acceleration, rotation and even

deformation related information. The research of F. S. Gayzik [10] built a Computer Aided Design (CAD) model for a full body in terms of a “man” seated in a car in order to processing Finite Element Analysis (FEA) and subsequently investigating the biomechanics during crash induced injuries. According to the results of this experiment, this full body CAD model can represent nearly 50% male. During this experiment, the software “Mimics Innovation Suite” was used to convert the 2D anatomy data of MRI and Computed Tomography (CT) image of every detailed structure to the 3D model. The final model included skeletal system, organ systems, muscular components, Ligamentous, and cartilaginous components and even skin components. With the help of post processing software such as ANSYS, the impact conditions can be given to the model such as the force, stress or the moment. However, there are still some shortcomings of this kind of method. First of all, parameters of the structures are very difficult to be given to the model especially for the complicated soft tissue, such as brain consisting of different parts (white matter, grey matter) with different physical properties, which means the parameters of each part of the brain should be given individually in computer which is very difficult to set up. Second, the causes of TBI usually are related to some situation that are complicated such as blunt impact and blast wave which can’t be presented perfectly during the post process with just few parameters set up, so the simulation results are not significant compared with the real situation.

Tagged MRI related technique has been widely used recently by most of the researchers who investigated the brain displacement and deformation during TBI.

With the help of Harmonic Phase (HARP) Technique, the motion information can be extracted from the tagged MRI data, in other words, during the TBI research, those tagged lines can move with brain tissue, so the information of the deformation can be obtained through the movement of the tagged lines [11]. For example, P.V. Bayly[12] and his research team found there was compression in front regions and stretching in posterior regions of the brain tissue during mild acceleration using tagged MRI technique to find the strain tensor with the tagged lines. Y. Feng and his colleagues developed a measurement to investigate the relatively displacement and deformation of human brain during mild TBI using MRI and digital image analysis [13], which contributed to the study of the boundary conditions of the skull to the brain. Another example can be shown by the study of Andrew K. Knutsen and his team in Johns Hopkins University [14], who optimized the traditional tagged MRI method, during which a single subject need to process 72 to 144 head rotations for obtaining deformation data with a single slice of image, with an enlarging of the subject number to 3 resulting in significant reduction of the cycle time of obtaining the deformation data. The tagged MRI technique is the most popular method those days in terms of the investigation of the kinematics of TBI, because comparing with other methods such as animal experiment and computational simulation, tagged MRI is much more visualized and accurate. However, there are still some limitations of this method. Firstly, the brain deformation with TBI usually can be regarded as a kind of spatial and temporal deformation, the temporal resolution of the image study should be improved especially when it comes to blunt injury or blast injury which require high

temporal resolution to achieve. Second, even if the increasing of the subject number can reduce cycle time, a much more sufficient and fast way to obtain deformation data is required.

Except tagged MRI technique, high speed biplanar x-ray is another popular imaging tool used for brain deformation measurement. This can be proven by the research of W.N. Hardy [15], who measured displacement data of cadaver brains with respect to skull during acceleration using bi-planar x-ray technique with speed from 250 frames/s to 1000 frames/s. However, the limitation of the spatial resolution and the difficulty for differentiating brain tissue properties of a living subject are still unsolved.

In conclusion, animal experiment, computational simulations, tagged MRI technique and high speed biplanar x-ray have truly contributed to the study of the brain deformation during TBI with different advantages and emphasis, however, there are some vital limitations of all of the methods above: the inability of simulating the real impact during TBI such as blast wave and blunt impact, and the restriction of collecting deformation data instantly and accurately due to the restriction of capturing the instant impact to the brain tissue.

1.4. Continuum Analysis in Deformation Measurement

It is widely accepted that the principle of Continuum Mechanics is a very useful tool for the analysis of spatial and temporal deformation of brain tissue in terms

of TBI, which mainly deals with the analysis of kinematics of a continuous mass instead of discrete single unit [16].

When an external force impacts on a continuum mass, displacement of which will appear including rigid body movement and inside deformation. First of all, the whole rigid body will displace with translation and rotation but the shape and size of which will not change; Second, due to the impact, there will be an inside deformation leading to a different configuration of the shape and size of the subject which can be described as deformed state comparing with initial state (unloading), which can be described as undeformed state of the subject.

Actually from the particle level, the reconfiguration of continuum mass is caused by the dislocation of every relevant particle in the mass, the dislocation od particles can be represented using vectors, which can be called “Displacement Fields” [17], a vector field of displacement vectors for particles inside the body is used to build the relationship between the deformed and undeformed states. It is common that $\kappa_0(Ɓ)$ usually is used to represent the undeformed reference configuration, and current configuration is represented by $\kappa_t(Ɓ)$ (Figure 1.2). It is widely accepted that the deformation gradient, which usually represented by F,is used to connect the deformed (x) and undeformed (X) state[18].

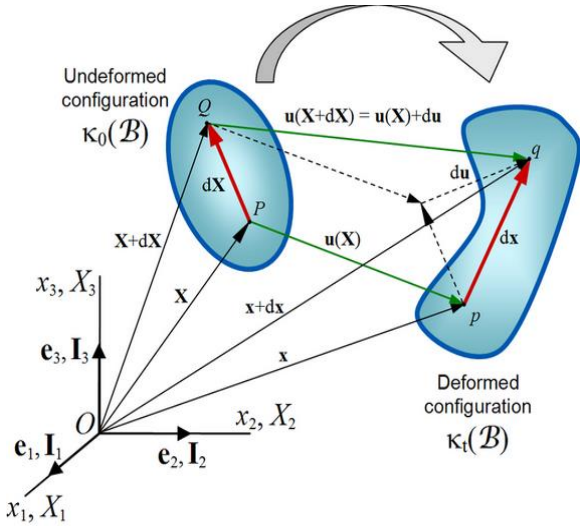

Figure 1.2 Displacement combining both of rigid body displacement and deformation of a continuum body. e_1, e_2,e_3 show the coordinate system and I_1, I_2,I_3 represent the unit vectors along X, Y and Z direction; Vector PQ represents the undeformed configuration κ_0 (Ɓ), and vector pq represents the deformed configuration κ_t(Ɓ); X and "X+dX" represent deformed vectors (OQ, OP) with respect to original point O, x and "x+dx" represent deformed vectors (Oq, Op) with respect to original point O; Displacement between any points can be defined as the difference between x and X, which generally using u to represent; In Figure 1.2, the displacement of point Q to point q, which is "u(X+dX)" can be represented by the sum of u (X) and du. In addition, t means the time interval between the deformed and undeformed states.
Source:https://en.wikipedia.org/wiki/Finite_strain_theory#/media/File:Displacement_of_a_continuum.svg (access on March 16, 2016).

The gradient function can be described as differentiation of the function respect to every component of the coordinates and during which both of x and X represent the vectors from the origin to their relatively points as follows:

$$\nabla f(x) = \left(\frac{\partial f}{\partial x_1}, \frac{\partial f}{\partial x_2}, \frac{\partial f}{\partial x_3}\right) \tag{1.1}$$

The deformation gradient F is the derivative of every component of deformed vector x to every component of undeformed vector X:

$$F_{ij} = x_{i,j} = \frac{\partial x_i}{\partial X_j} = \begin{bmatrix} \frac{\partial x_1}{\partial X_1} & \frac{\partial x_1}{\partial X_2} & \frac{\partial x_1}{\partial X_3} \\ \frac{\partial x_2}{\partial X_1} & \frac{\partial x_2}{\partial X_2} & \frac{\partial x_2}{\partial X_3} \\ \frac{\partial x_3}{\partial X_1} & \frac{\partial x_3}{\partial X_2} & \frac{\partial x_3}{\partial X_3} \end{bmatrix} \tag{1.2}$$

The information of deformation will be obtained after the calculating of the deformation of the gradient tensor. Indeed the rotation and deformation information can be represent from F, it is still necessary to find a way to divide the two components if the further study of stress and strain is required, cause the rotation is not relevant to the calculation of stress and strain. The knowledge of Polar Decompositions is required to partition the rotation and deformation, where U represents the stretch tensor can be used for further study for calculating strain and stress; R represents the rotation matrix and F represents the deformation gradient read from left to right as follows:

$$F = R \cdot U \tag{1.3}$$

Then through transformation of product with transpose of F, the equation between F and U can be obtained as follows:

$$F^T \cdot F = (R \cdot U)^T \cdot (R \cdot U) = U^T \cdot R^T \cdot R \cdot U \tag{1.4}$$

$$R^T \cdot R = I \tag{1.5}$$

$$F^T \cdot F = U^T \cdot U \tag{1.6}$$

Here U is regarded as a symmetric matrix so the transpose of which is equal to the value of U, so the U can be presented as follows, which is stretch tensor combing the information of both shear and normal deformation:

$$U^T = U \tag{1.7}$$

$$F^T \cdot F = U^2 \tag{1.8}$$

$$U = \sqrt{F^T \cdot F} \tag{1.9}$$

Generally, the product of stretch tensor U and its transpose U^T can be described as Right Cauchy-Green Deformation Tensor, usually which can be represented by C and this tensor actually excludes the influence of rotation:

$$C = U^T \cdot U = F^T \cdot F \tag{1.10}$$

Finally, the further examination of strain can be developed using Lagrangian strain tensor E as follows, where I represents the identity matrix:

$$E = (F^T \cdot F - I)/2 \tag{1.11}$$

In addition, when it comes to 2D field, the Lagrangian strain tensor (1.11) will provide the changing of shape and size of finite element as follows, where ε_{xx} represents the strain in x direction, ε_{yy} represents the strain in y direction, and the

rest of the two elements in this matrices: ε_{xy}, ε_{yx} represent the shear strain in both two directions as follows:

$$E = \begin{bmatrix} \varepsilon_{xx} & \varepsilon_{xy} \\ \varepsilon_{yx} & \varepsilon_{yy} \end{bmatrix} \tag{1.12}$$

Experimentally, the method of continuum analysis has been shown to be an accurate and efficient tool to study the deformation patterns at the cellular level. (Figure 1.3) [19].

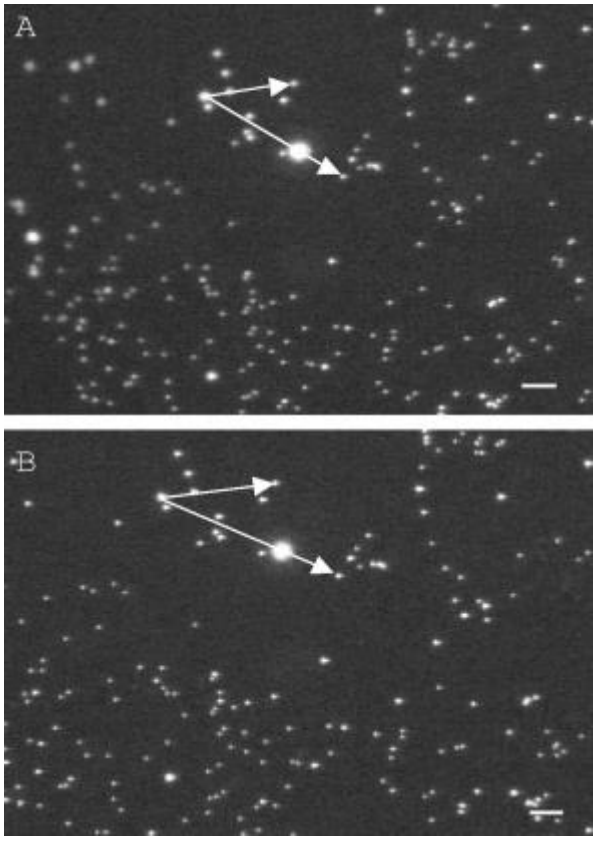

Figure 1.3 Snapshots from fluorescence microscopy view (Scale Bar=50μm) of both deformed and undeformed states of silicon substrates sticking with fluorescent beads (0.5μm, Polysciences, Warrington, PA). In every of the two states, there are two vectors created using 3 points, after collecting data, the 2D deformation gradient and strain tensor are obtained through continuum analysis in this experiment.
Source: Bryan J. Pfister et al. (2003).

1.5 Conclusion

It is widely accepted that TBI is a serious problem and the deformation of brain tissue resulting from the blunt injury, blast wave can really be key to understanding biomechanics of head injury. Although animal experiments, computational simulations, high speed x-ray and tagged MRI technique have been used for brain deformation measurement, there are still some limitations such as the inability to mimic the real conditions including blunt injury, and the limitation of

deformation data acquisition. Using knowledge of continuum analysis to create deformation and strain tensor has been proven to be an efficient way to investigate the deformation pattern of brain tissue. Following chapters will describe the objective of this experiment and a series of experiment steps, results and discussion.

CHAPTER 2

OBJECTIVE

The objective of this thesis was to develop a new method to measure deformation pattern of brain tissue in terms of blunt injury. First of all, an impact test was developed to mimic the real situation of blunt injury based on dummy head model coming from previous study. Second, the 2D displacement data of brain model was captured by high speed video imaging system and collected by 3D kinematic reconstruction software ProAnalyst (Xcitex, Inc.). Then using continuum analysis, the 2D strain tensor and principal strain was calculated with Matlab (2015a). Finally, the results of the strain would be compared in terms of 3 different variables including impact velocity, impact location and concentration of gel used for creating the head model. A method of presenting the results of spatial location would be developed in order to finding deformation pattern within different variable condition.

CHAPTER 3

MATERIALS AND METHODS

3.1Design of Head Model

There are many ways design and construct a head model including 3D printing, casting, and real head model using cadaver material, which is much more precisely and can represent data much more convincingly comparing with the other two techniques. However, just like the 3D printing technique, a head model related to cadaver is more expensive than casting. In this experiment, a casting design based on previous study was used to create the head model (Table 3.1).

Table 3.1 Information for Materials used for Creating Head Models

Materials	Supplier
12 A-102491 Budget Life-Size Skull Anatomy Model	Anatomy Warehouse, IL,
Synthetic Ballistic Gel	Clear Ballistics, Ark
Neck of Hybrid III Anthropomorphic Test Device (ATD)	Humanetics, MI
Band Saw	Scheppach, Germany
Drill Press	Westward, CA
Black Spray Paint	Rust-Oleum, IL
Black ABS Panel	Interstate Plastics, CA
White Silicone Lubricant	WD-40,CA

3.1.1 Casting Design of the Head Model

The casting design can be divided into several steps: First, life size skull replicates(Anatomy Warehouse, IL) were cut by a band saw (Scheppach, Germany) to create a sagittal cut at roughly 5/8 of the skull. This was performed on two skulls. Second, ballistic gels (Clear Ballistics, Ark) of 10% and 20% concentrations were melted as per manufacturer instructions and poured to within 1 cm of the sagittal cuts. These gels were then allowed to solidify overnight. Third, black spray paint (Rust-Oleum, IL) was used in conjunction with a 3-D printed ABS grid of holes in order to create a pattern of markers on the ballistic gel. Fourth, after the markers became dry, a new layer of gel was created just like step 2 above, which was placed

on the top of the markers in order to prevent the markers adhering to the cover panel. Fifth, a white silicone lubricant (WD-40, CA) was used to build another layer between the gel and the cover panel in order to reducing the friction and avoiding the sticking phenomenon. Finally, a cover panel of polycarbonate was cut to shape using the band saw (Scheppach, Germany) to seal the head model using silicone caulk (Figure 3.1).

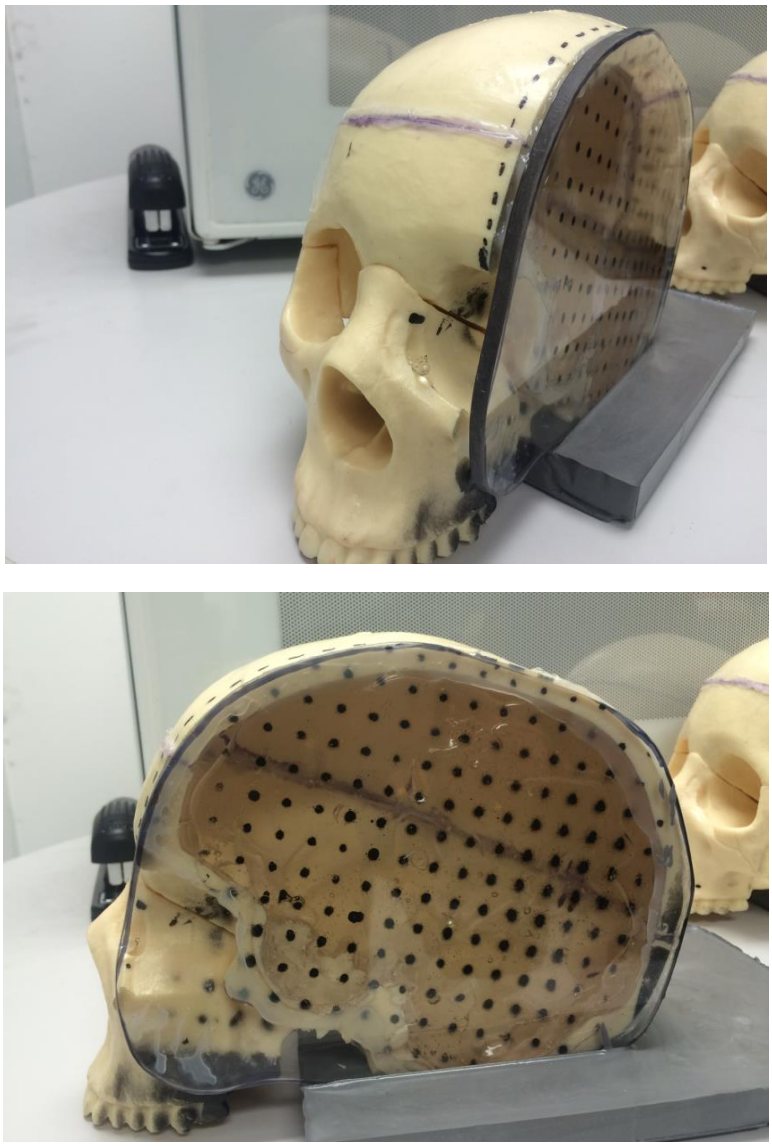

Figure 3.1 The left and front view of the head model structure built using casting technique and black paint markers.

3.1.2 Assembly of Head Model and Neck

In this experiment, hybrid III anthropomorphic (Humanetics, MI) was connected to the skull (Figure 3.2). The bottom of the skull was encased in machinable epoxy and allowed to cure overnight. Then a drill press tool (Westward, CA) was used to drill three holes in this epoxy layer, after which the head model was connected with the neck by screws. (Figure 3.3)

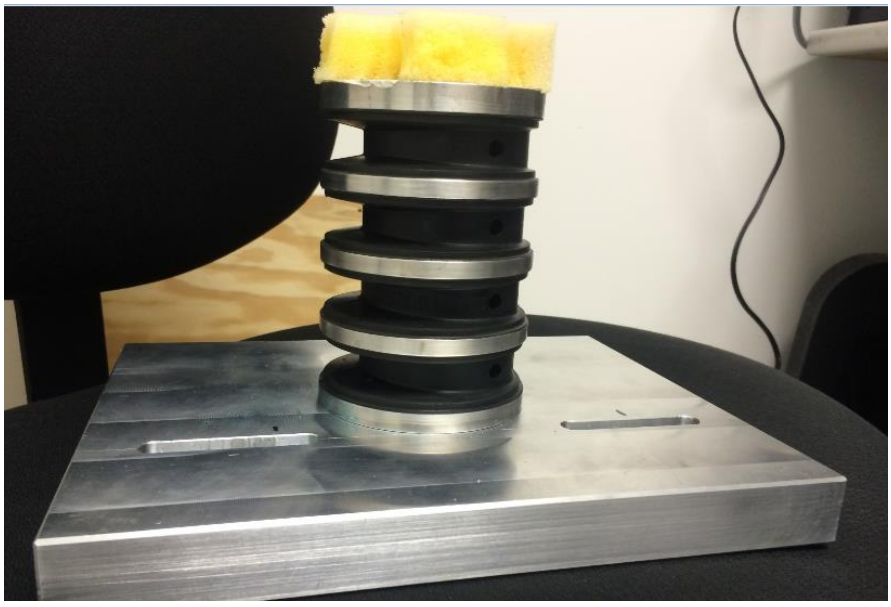

Figure 3.2 The neck of hybrid III anthropomorphic test device (Humanetics, MI) used for connecting the impact tower and head model in this experiment.

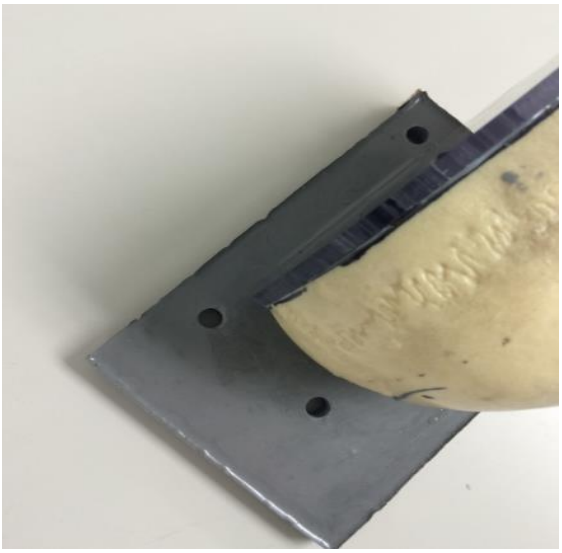

Figure 3.3 The layer of aluminum used to connect the head model and the neck.

3.2 Drop Impact Tower Test and High Speed Video Imaging System

A head injury biomechanical system consisting of an impact testing machine (CadexInc, Canada) and a high speed 3D video imaging system (Figure 3.4) of

UX100 M3 cameras (Photron, USA) was used to mimic the blunt impact and capture the video during the impact.

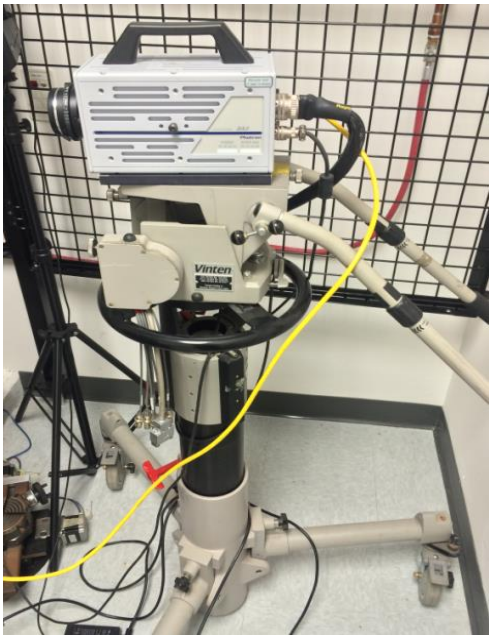

Figure 3.4 The high speed 3D video imaging system of UX100 M3 cameras (Photron, USA) was used to capture the movement of black markers on the surface of the sagittal plane in term of the head model with a speed of 1000 frames/ second.

In this experiment, an Uniaxial Impact Monorail Machine (Model : 1000_00_MIMA) was used to animate the uniaxial impact to the head model, which usually was described as a free fall guided impact machine for attenuation evaluation in lots of similar biomechanic related tests(Figure 3.5).

Figure 3.5 The basic structure of the impact machine includes 6 major features: Drop follower (1); Soft release system (2); Electronic encoder measuring system (3); Velocimeter, which can be regarded as the time gate used for speed measuring (4); Quick and easy interchangeable anvils (5) and remote control (6), which usually was used to input different value of the height, and start or stop the test during the experiment.

After the assembled neck and head model was connected with the anvil of the impact machine by four screws. Impact test was started and could be divided into several steps. First of all, through the remote control system, the impactor was lifted into a specific position with the height, and obtained potential energy (PE). Secondly, the impactor was released and the potential energy gradually was converted into kinetic energy ($E_к$). At the end, the energy of the blunt impact was transferred to the head model, so the brain and skull of the head models were deformed by the impact and the relative velocity (ΔV) could also be obtained.

$$PE = mgh \tag{3.1}$$

$$E\kappa = \frac{1}{2}mv^2 \tag{3.2}$$

$$\Delta V = \sqrt{2gh} \tag{3.3}$$

During the experiment of the impact test, 3 major variables were used for finding the deformation pattern in terms of the sagittal plane of the brain including impact velocity, impact location and concentration of ballistic gel, which was used for mimicking the brain tissue of the head model.

To begin with, the impact machine would provide different impact velocities with different height from the impactor (Figure3.6) to the head model according to the formula above (Table 3.2).

Table 3.2 Different Impact Heights with Different Impact Velocities.

Height (cm)	25	9
Velocity (mile/hour)	5	3

Second, different two head models with different concentration of gel including 10% gel (10% gel was solid, 90% gel was solvent) and 20% gel (20% gel was solid, 80% gel was solvent) were hit by the impact machine. The reason for choosing this parameter as a variable is that according to previous study[20], 20% gel have acoustic properties similar to water (a common stand in for brain).

Figure 3.6 The impactor with head shape was used in this experiment to mimic the blunt impact to the head model. The weight of the impactor is 10 pounds, which is close to the weight of a human head.

In addition, the different impact locations in terms of crown of head, fore head and even back head were also believed having significance in the study of brain deformation pattern with blunt injury, because in reality all of the situation would happen, especially for the brain injury with forehead impact, which was usually observed in sports games. In this experiment, the impact locations of both crown and fore head were chosen as the variables. A shelf with 45 degrees angle was created to provide the specific position for the impact test of forehead (Figure 3.7), and for each of the variables, there were 3 hits under different condition, and the total number of hits was 15 (Table 3.3).

Table 3.3 Summary of Three Variables and Hit Times used in Impact Test.

Percent of gel	Impact velocity (miles/hour)	Impact location	Hit times
20%	3	Crown	3
20%	3	Forehead	3
20%	5	Crown	3
20%	5	Forehead	3
10%	3	Forehead	3

During the same time, the impact processes were captured by the high speed video camera system in the lab at 1000+ frames/sec. In this experiment, most of the data coming from the impact machine such as the velocity and force would not be paid more attention to. The most important data collected in this experiment are the impact videos of the head models captured by the high speed camera system, which provided useful impact data for this experiment and would be converted into displacement data in next part of this experiment using 3D reconstruction software.

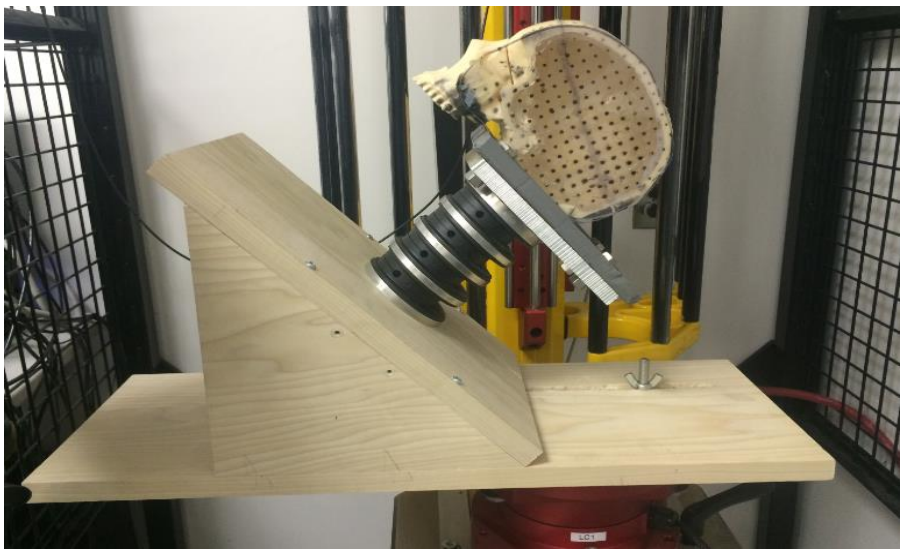

Figure 3.7 The shelf with 45 degree angle was used for the impact test of forehead position.

3.3 3D Kinematic Reconstruction and Data Acquisition

After the experiment of measurement of head injury biomechanical system, software ProAnalyst (Xcitex, Inc.) was used to extract the displacement data of the markers in the head model from the high speed camera video. ProAnalyst has been widely used for measuring all kinds of parameters including displacement, acceleration and velocity in term of moving objects. In this experiment, ProAnalyst was used for tracking the displacement coordinates of the brain markers during the impact process, and can be divided into several steps. First of all, parameters of brightness and contrast of video imported from the high speed video camera was adjusted using the tool of image processing in ProAnalyst, otherwise the video obtained from the high speed camera was too dim because of the very high film speed (1000 fr/s) to capture the movements of the black markers (Figure 3.8). Second, with

the help of the calibration tool, a 2D coordinates system was set up, and a calibrate scale of 0.375 inch was given to the distance between two markers(Figure 3.9). Third, the 2D features, in this experiment which refer to markers, were tracked using the feature tracking tool. A total number of 90 markers were chosen as a 10×9 matrix (Figure 3.10) for tracking manually. Finally, the displacement data in terms of coordinates values (x, y) of the 90 markers were collected based on time frame and exported as the format of excel (Figure 3.11).

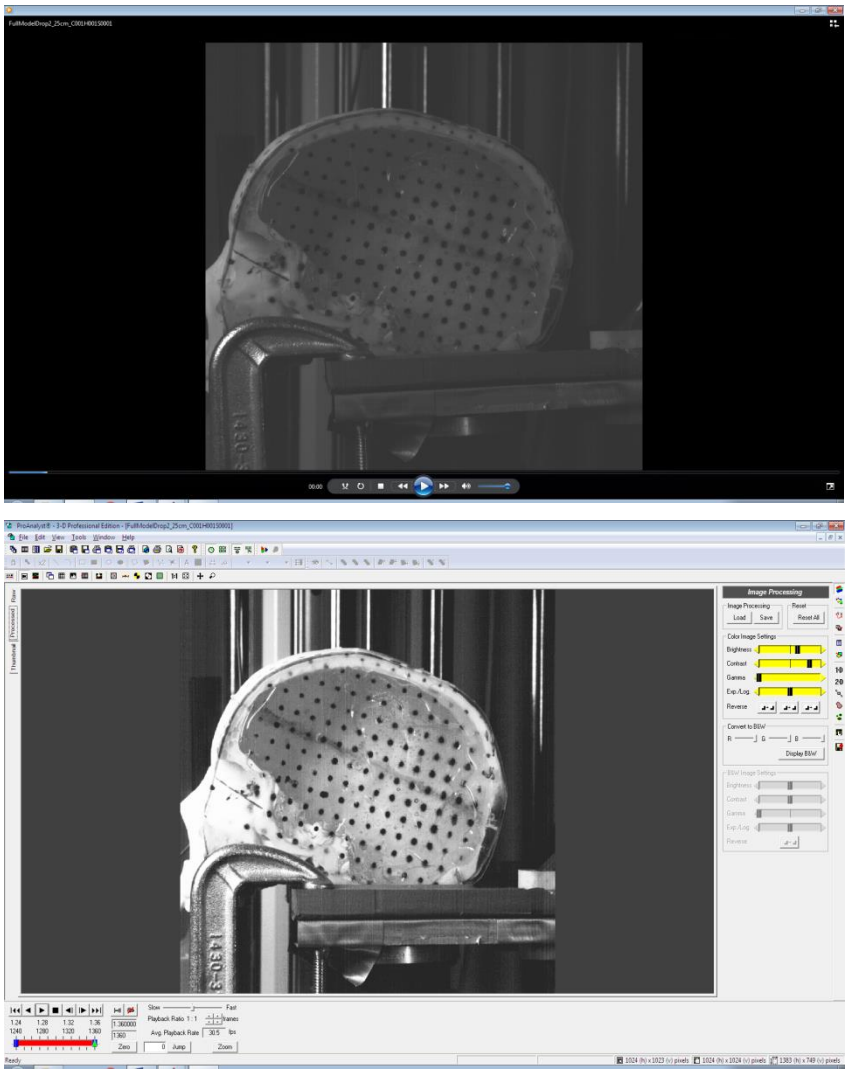

Figure 3.8 The comparison between the original video obtained from the high speed video camera system and the filtered video after imaging process in the ProAnalyst, which prove that the imaging process is necessary and through which the movement of black markers on the surface of the sagittal plane of the head model could be much more easily to track.

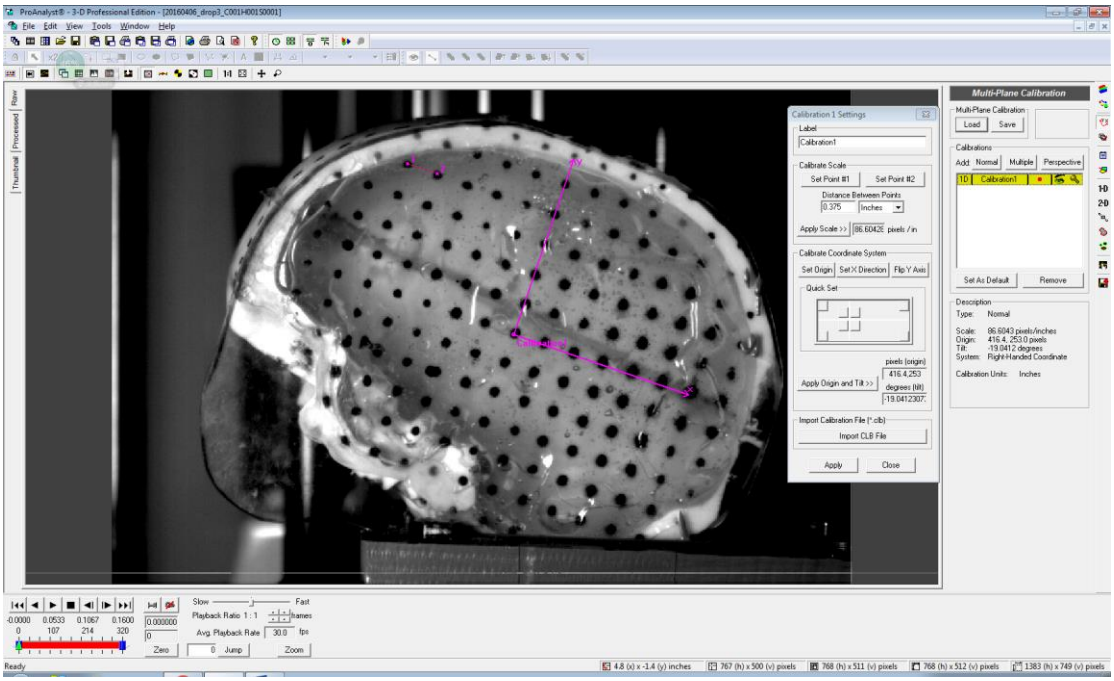

Figure 3.9 This figure shows the calibration process using ProAnalyst, during which the center point of all of the markers was selected as the original point to set up the 2D coordinates system, and the distance between point 1 and point 2 above was given value of 0.375 inch, which was the average spacing between two markers and was measured before the impact test using ruler.

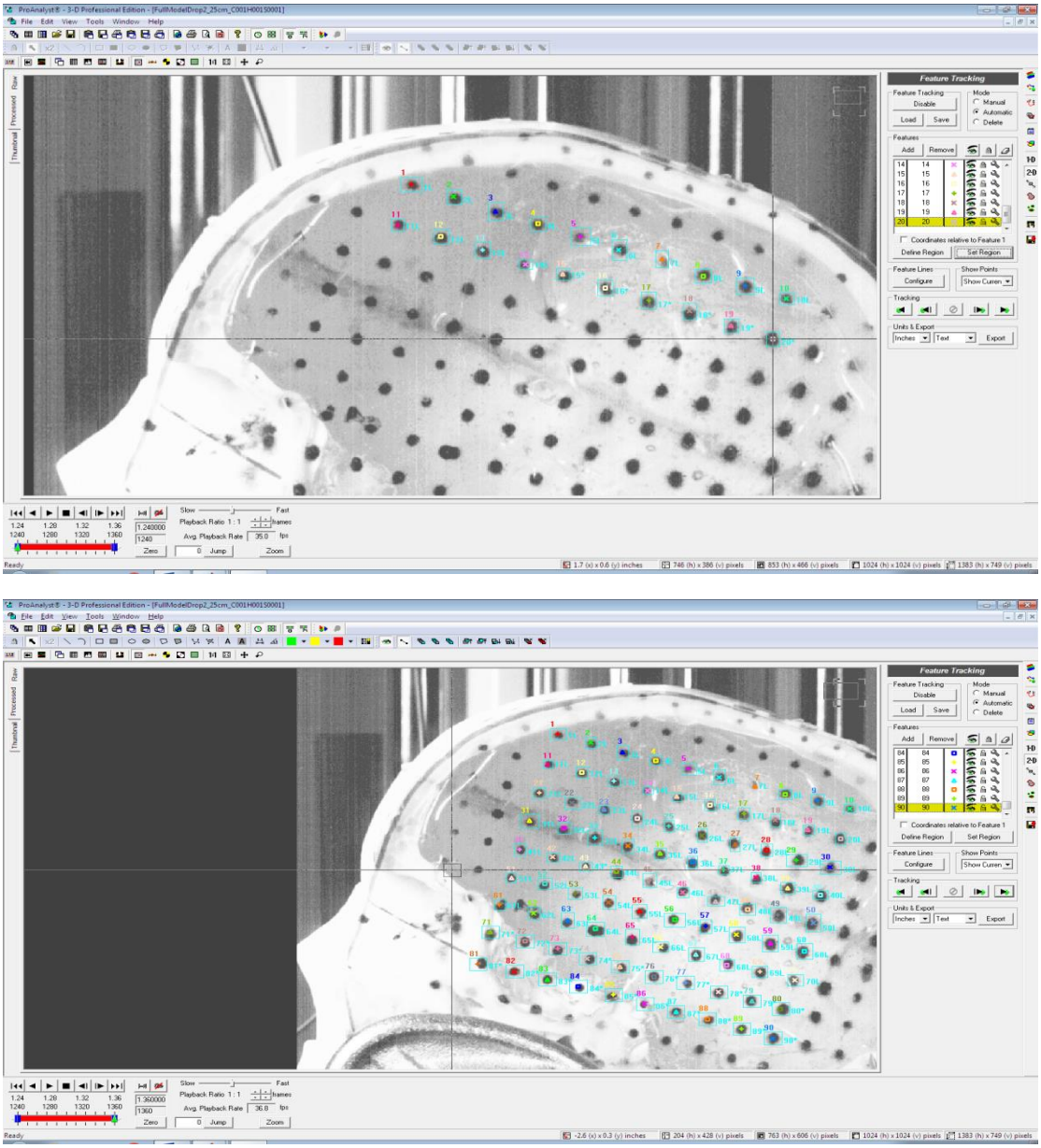

Figure 3.10 The 2D tracking process using ProAnalyst, through which the movements of 90 markers were tracked, this is the most important process providing original displacement data and were further used for obtaining deformation and strain information in terms of time dependent and space dependent data.

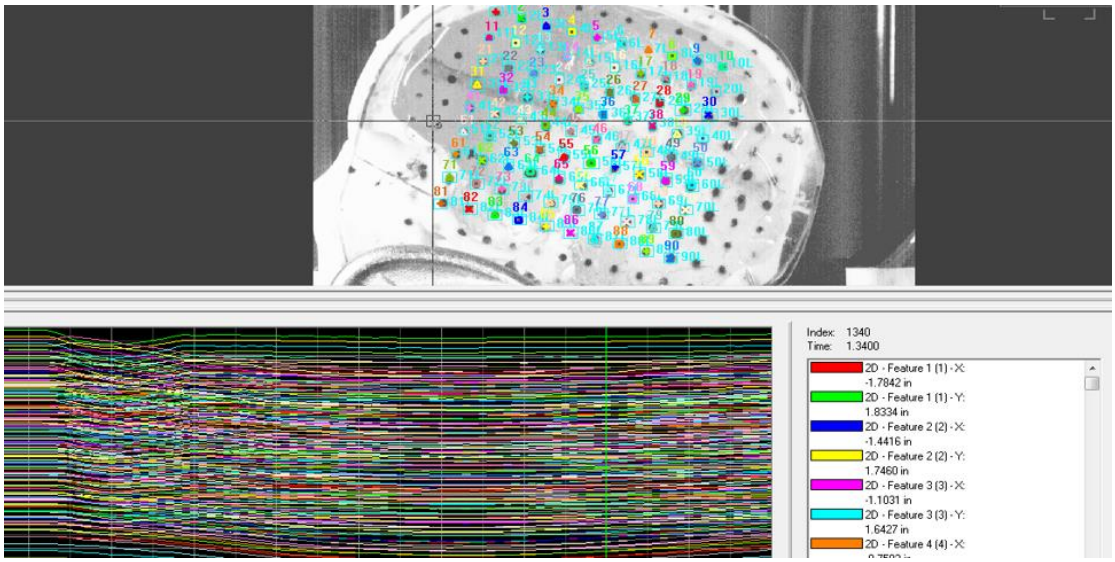

Figure 3.11 The final step of using ProAnalyst was to extract the real coordinates data of x and y value from the movements of 90 markers during the blunt impact process along a timeline.

3.4 Calculation of Strain Tensor and Principal Strain

The coordinates data of x and y values extracted from ProAnalyst were imported into Matlab, after which, 2D strain tensor and principal strain would be would be calculated with the basic knowledge of continuum analysis.

The 90 markers with equal distance to each other can form 79 squares ordered from left to right, top to bottom. Each of the 79 squares was composed by 4 markers at vertex (Figure 3.12). Within each square, the displacement data of 3 of the 4 markers located in the vertex in terms of the x and y value of the coordinates were converted into vectors described as "$dx^{(h)}$", which is the horizontal vector, and "$dx^{(p)}$", which is the perpendicular vector (Figure 3.13). And both $dx^{(h)}$ and $dx^{(p)}$ represent the deformed state, the undeformed configurations were presented by $dX^{(h)}$ and $dX^{(p)}$ which were measured and calculated in terms of the first time frame of the video.

According on the information above, the deformation gradient F, which is a series of 4D matrix including the information of deformation along x direction, y direction and shear deformation within each square was calculated as follows:

$$\left[(dx^h)'\ (dx^p)'\right] = F\left[(dX^h)'\ (dX^p)'\right] \tag{3.4}$$

$$F=[(dx^h)^T(dx^p)^T] \times [(dX^h)^T(dX^p)^T]^{-1} \tag{3.5}$$

The right Cauchy-Green tensor was used to eliminate the rotation effects which were definitely not significant for making contributions to the deformation and strain calculation.

$$C=F^T \times F \tag{3.6}$$

After the calculation of the right Cauchy-Green tensor, in this experiment Lagrangian strain tensor "E" was obtained by the following formulas during which "I" represents the identity matrix, and according to the matrix of E, the information of normal strain from x direction represented by ε_{xx}, y direction represented by ε_{yy} and the shear strain, which can be represented by $\varepsilon_{yx}\ and\ \varepsilon_{xy}$ can be obtained for each square along the timeline.

$$E = (F^T \cdot F - I)/2 \tag{3.7}$$

$$E = \begin{bmatrix} \varepsilon_{xx} & \varepsilon_{xy} \\ \varepsilon_{yx} & \varepsilon_{yy} \end{bmatrix} \tag{3.8}$$

After the calculation of the strain tensor, it is necessary to calculate the principal strain($\varepsilon_1,\ \varepsilon_2$) and maximum shear strain (γ_{max}) in this experiment using the formulas as follows:

$$\varepsilon_1 = \frac{\varepsilon_{xx}+\varepsilon_{yy}}{2} + \sqrt{\left(\frac{\varepsilon_{xx}-\varepsilon_{yy}}{2}\right)^2 + \left(\frac{\varepsilon_{xy}}{2}\right)^2} \tag{3.9}$$

$$\varepsilon_2 = \frac{\varepsilon_{xx}-\varepsilon_{yy}}{2} - \sqrt{\left(\frac{\varepsilon_{xx}-\varepsilon_{yy}}{2}\right)^2 + \left(\frac{\varepsilon_{xy}}{2}\right)^2} \tag{3.10}$$

$$\frac{\gamma\ max}{2} = \sqrt{\left(\frac{\varepsilon_{xx}-\varepsilon_{yy}}{2}\right)^2 + \left(\frac{\varepsilon_{xy}}{2}\right)^2} \tag{3.11}$$

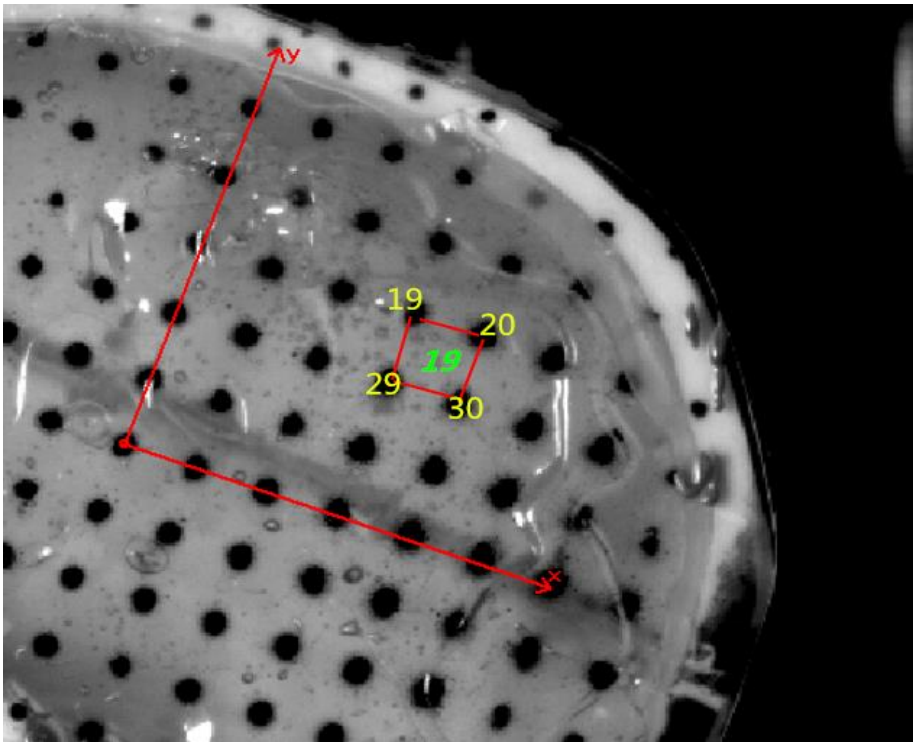

Figure 3.12 This figure indicates the numbering of the markers and the squares. The yellow numbers including "19, 20, 29, 30" indicate the 4 of the 90 black markers, and the number of "19" with green color indicate the 19th square location of the 72 squares.

Because the whole experiment was time dependent and there are more than one square needed to be calculated the strain, so Matlab was used to build loop for the continuous calculating of the deformation gradient and strain tensor for all of the squares with timeline. At last the strain data coming from the head model with different were obtained through the Matlab programming (Appendix).

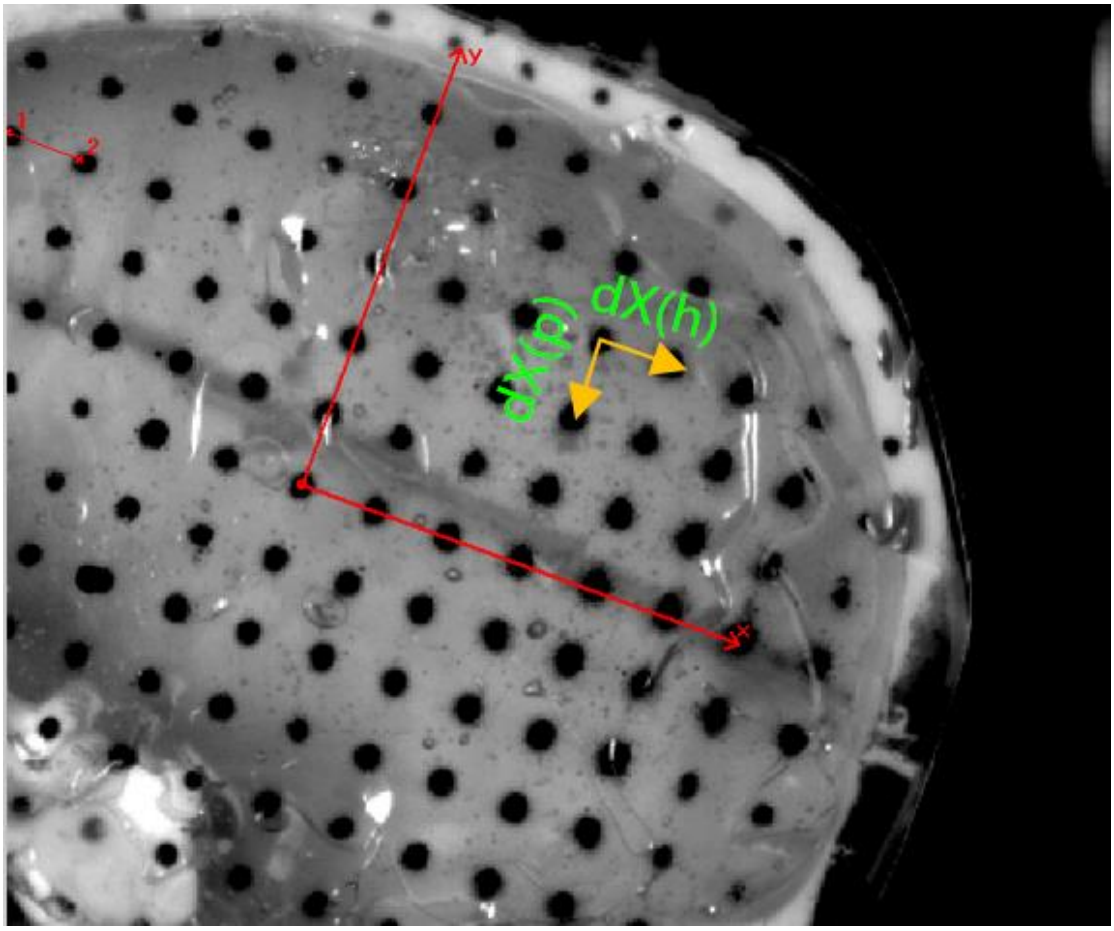

Figure 3.13 An example showing the two vectors used for creating the deformation gradient tensor including $dx^{(h)}$ and $dx^{(p)}$, following which the deformation gradient and strain tensor was created indicating the strain information of one of the 72 squares.

3.5 Presenting Results with Matlab and Minitab

Quantitative results including strain value and rise time of the principal strain and maximum shear strain were presented by interval plot (95%, CI for the mean) using Minitab 17.0. Spatial location results were presented using contour plot with the programming tool from Matlab, the coordinates (x, y) of each square center with respect to the origin, and strain values of 72 squares were calculated finally as input for creating contour plots (Figure 3.14). It was easier and convenient to use contour plot to visualize the deformation pattern.

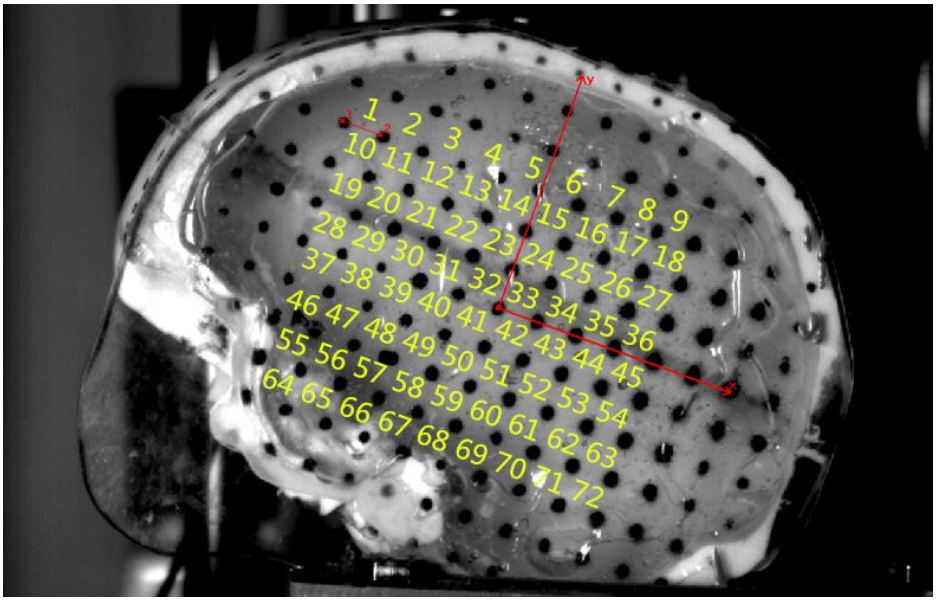

Figure 3.14 The numbers of 72 squares indicating the specific spatial location on the surface of the sagittal plane.

CHAPTER 4

RESULTS AND DISCUSSION

4.1 Comparison of Results with Different Impact Velocities

In this study, impact height, the perpendicular distance between the impactor of the impact machine and the injury head model produces a precise impact velocity was the first variable analyzed. 25 cm and 9 cm produced impact velocities of 5 mile/hour and 3 mile/hour as measured by the velocimeter of impact machine The reason for choosing this variable was the intention for mimicking the impact velocity closed to the reality in terms of impact injury, 5 mile/ hour was closed to the speed of running in the daily life, and 3 mile/hour was much more like walking. For this first set of experiments, the model with 20 percent gel and impact location of crown head was used to compare the results of different impact velocities, and all of the strain data including ε_1, ε_2 and γ_{max} (Table 4.1 and Table 4.2). In this study, the rise time (Figure 4.1) which indicated the time interval from start point of the rising to the end point of the peak value of maximum strain was also calculated using plot tool of Matlab. The results of strain value, rise time and spatial location would be analyzed next.

Table 4.1 Strain Value and Spatial Location Data of 20 Percent Gel Model with Crown Head Impact Position for 3 mph Impact.

	ε_1			ε_2			γ_{max}		
Rise Time(s)	0.004	0.005	0.005	0.0045	0.0045	0.006	0.005	0.005	0.005
Spatial Location	14	11	20	13	11	38	23	33	20
Strain Value	0.092	0.084	0.081	-0.116	-0.101	-0.107	0.187	0.162	0.155

Table 4.2 Strain Value and Spatial Location Data of 20 Percent Gel Model with Crown Head Impact Position for 5 mph Height.

	ε_1			ε_2			γ_{max}		
Rise Time(s)	0.0085	0.0065	0.007	0.006	0.005	0.004	0.006	0.0045	0.003
Spatial Location	20	23	14	23	13	13	13	5	10
Strain Value	0.163	0.165	0.161	-0.219	-0.171	-0.183	0.317	0.305	0.322

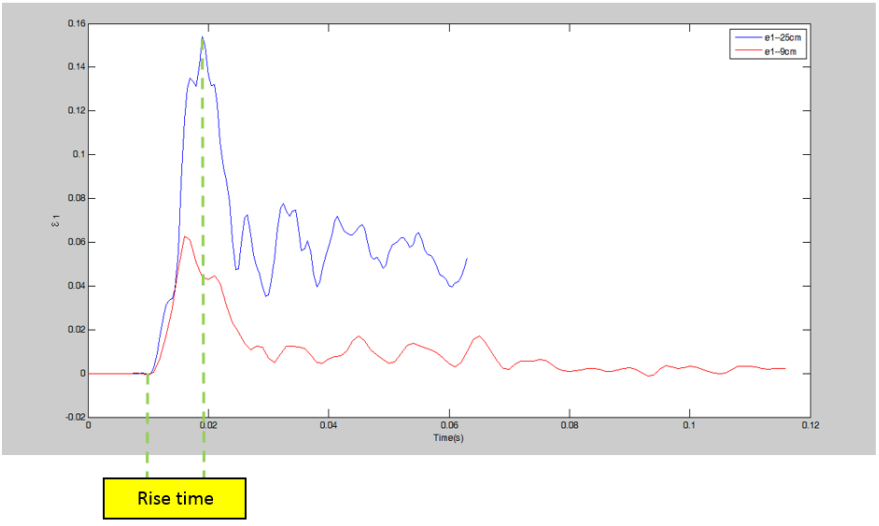

Figure 4.1 Definition of the rise time indicating the time interval from the start point of rising to the end point of the rising in terms of the strain value changing with the time went by.

Under the same other conditions including 20 percent gel and impact location of crown head, when it comes to the strain value, firstly it was obtained that the mean strain values of the 5 mph experiment are larger than the strain values of the experiment with the 3 mph impact height in terms of ε_1, ε_2 and γ_{max} (Figure 4.2). It really fit the reality because comparing with the impact height of 9cm, the height of 25cm lead to a higher impact velocity and larger kinetic energy (E_κ), and the larger E_κ of the impactor would be transduced into the head model and caused larger value of deformation and strain. Secondly, the magnitude of ε_1 is smaller than ε_2 in both of the 5 mph and 9 mph experiments indicating that in terms of the same impact location of crown head, models would be compressed much more other than stretching.

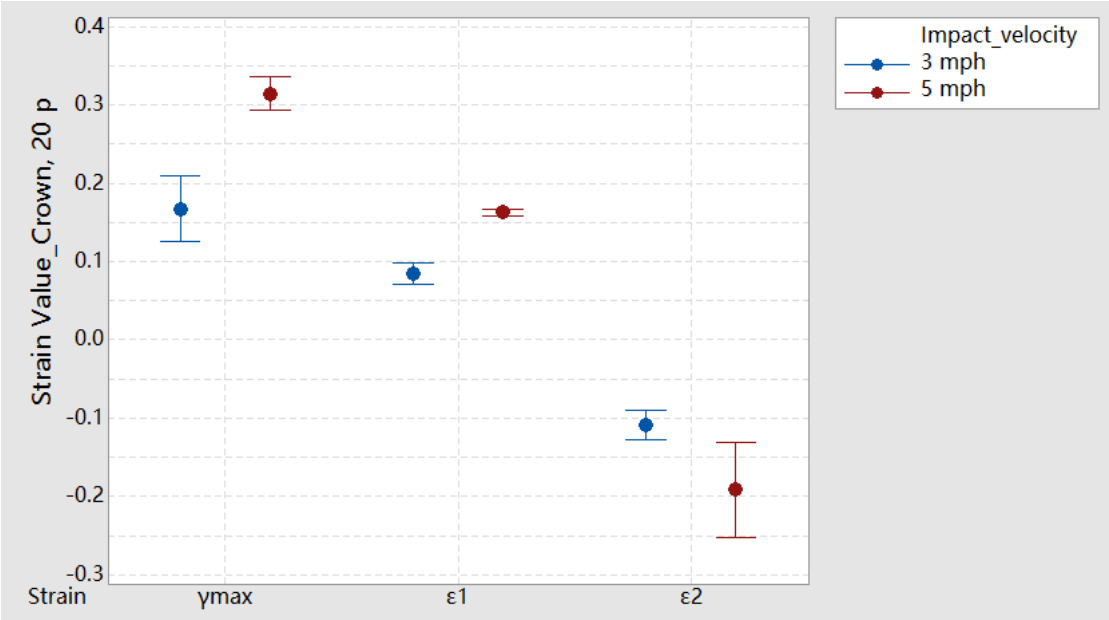

Figure 4.2 Strain value comparison between different impact velocities (5 mph, 3 mph) in terms of principal strain (ε_1 and ε_2) and maximum shear strain with 20 percent gel, impact position of crown, 95% CI for the mean.

It was found that comparing with the results of 9 cm, the rise time of 25cm in terms of ε_1 and ε_2 were significantly larger (Figure 4.3), which means that the strain with 25cm condition required more time to reach the peak value compared with the experiment under the condition of 9cm. This phenomenon can be ascribed as the larger energy the 25cm height produced need to be transduced to the skull, and it took longer for the strain to develop.

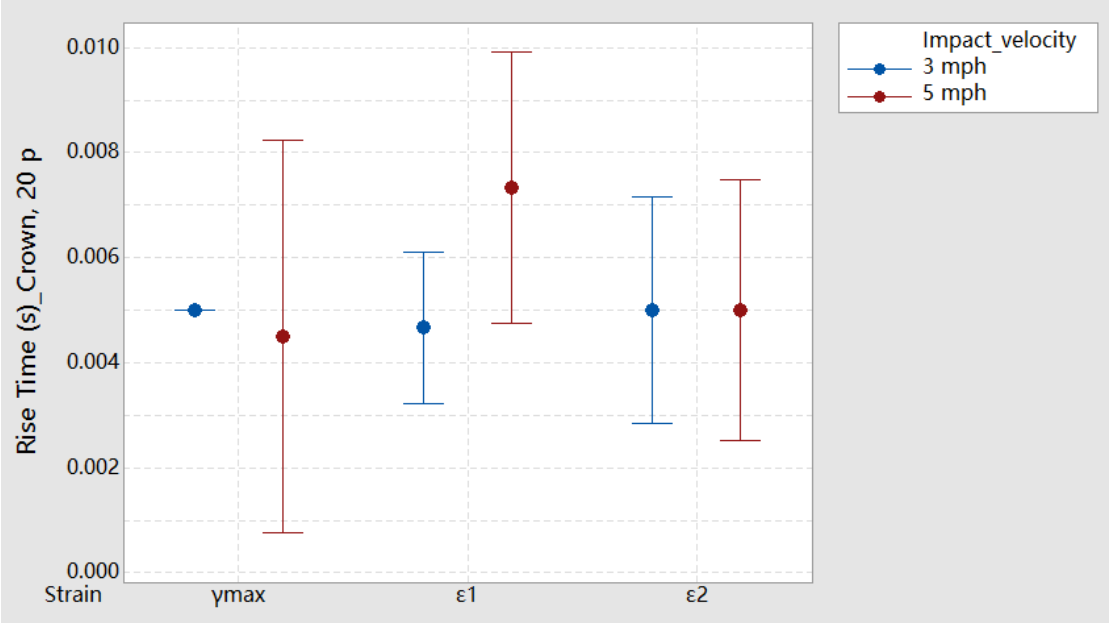

Figure 4.3 Rise time comparison between different impact velocities (5 mph, 3 mph) in terms of principal strain (ε_1 and ε_2) and maximum shear strain with 20 percent gel, impact position of crown, 95% CI for the mean.

In order to visually display the spatial location of maximum strain, the plane of the markers was divided into 4 quadrants (Figure 4.4) using the coordinate system set up in the calibration process using ProAnalyst. It was obtained that the spatial location of maximum strain values remained within the same quadrant, nearly all of which (10 of 12 values) occurred at the second quadrant, which was mostly close to the impact position (Figure 4.5). In terms of the contour plot (Figure 4.6) of all 72

squares, First of all, the results of higher impact height of 25cm shows a larger area of deformation, nearly all of the squares were deformed compared to the results of the 3 mph experiment.

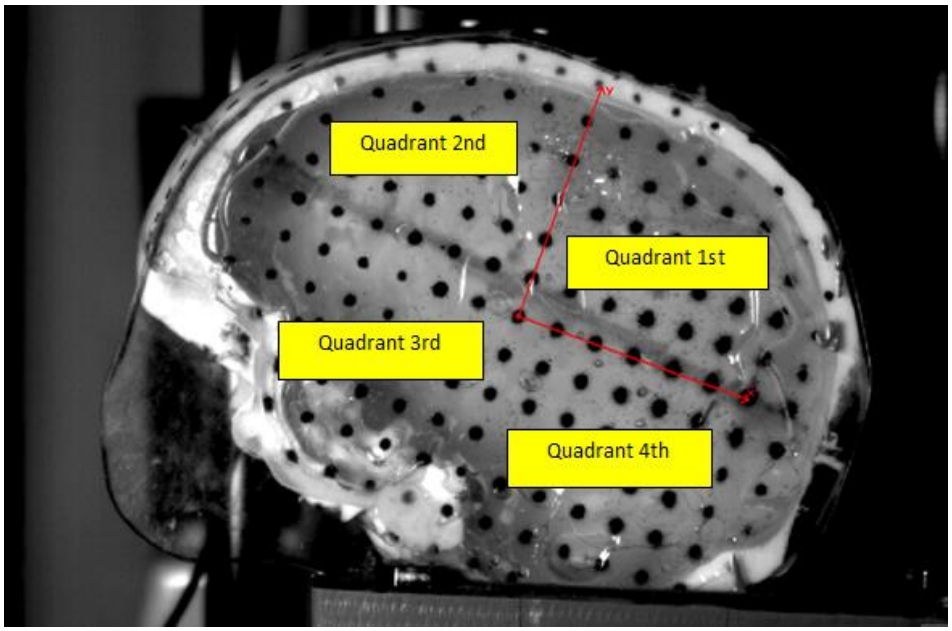

Figure 4.4 Four quadrants used for describing the specific location of maximum strain and deformation pattern with the coordinates system.

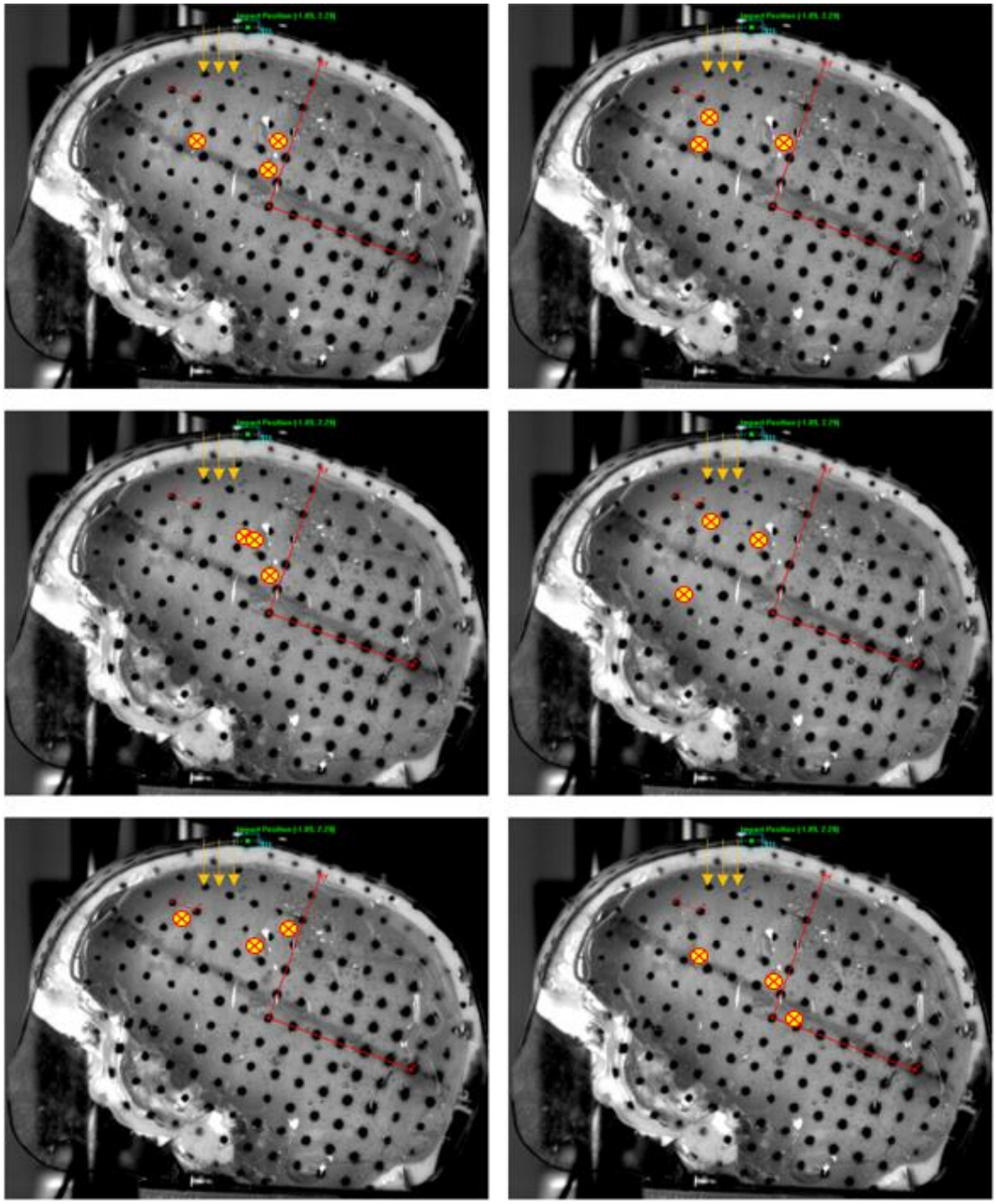

Figure 4.5 Spatial location comparison between different impact heights (25cm in first column, 9cm in second column) in terms of principal strain ε_1, ε_2 and maximum shear strain from top to bottom, with 20 percent gel, impact position of crown. Each yellow circle indicated the spatial location where maximum strain value appeared. And the impact locations were indicated by the yellow arrow.

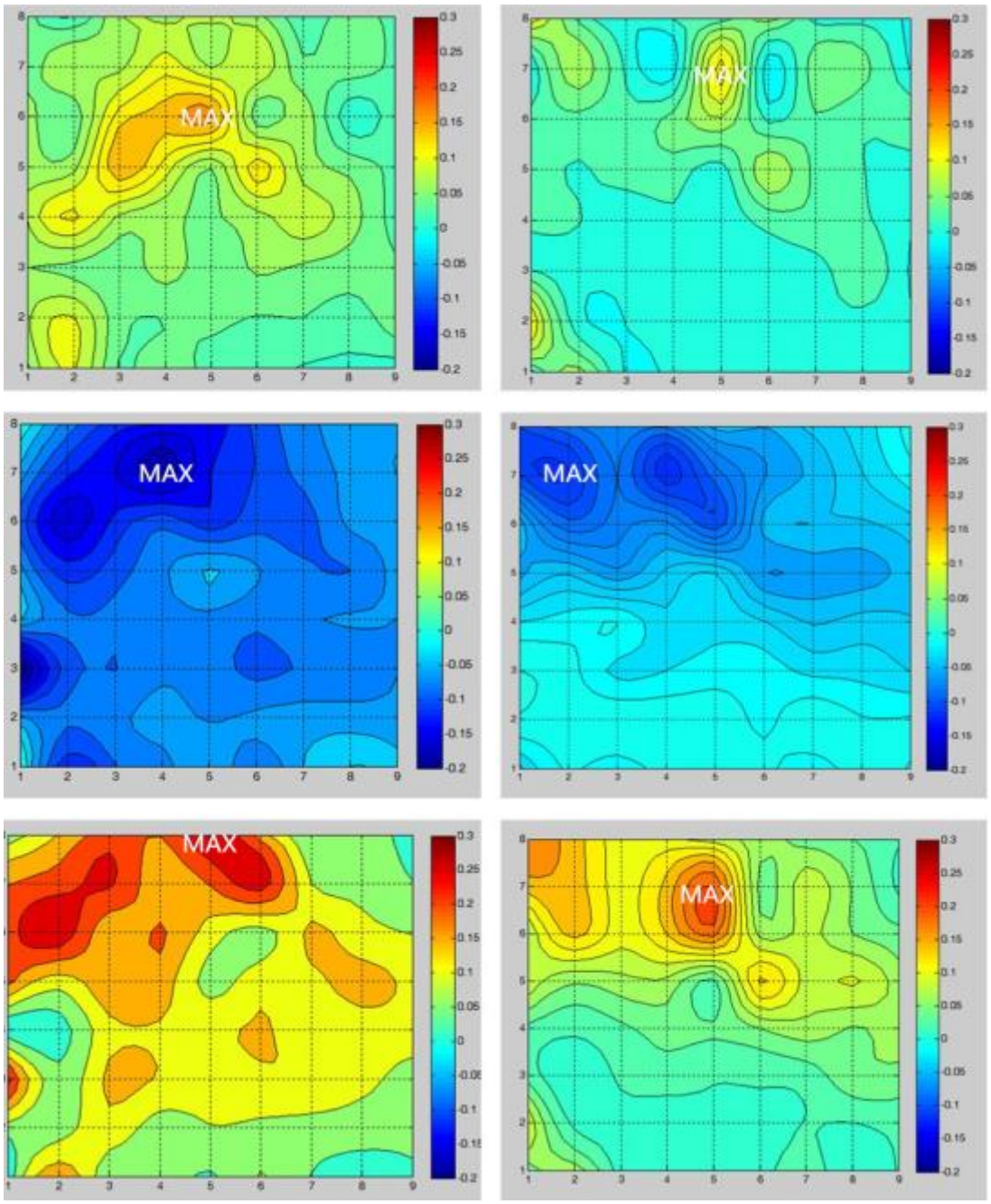

Figure 4.6 Comparison in terms of contour plotting all 72 squares between different impact heights (25cm in first column, 9cm in second column) in terms of principal strain ε_1, ε_2 and maximum shear strain from top to bottom, with 20 percent gel, impact position of crown.

4.2 Comparison of Results with Different Impact Locations

The second variable compared in this study is impact location. Different locations of crown of the head and forehead were chosen to be compared with each other (Figure 4.7). Choosing different impact locations as a variable was believed to be very helpful for investigating the different TBI situations in reality, especially the fore head impact injury is very common those days happened to athletes in sports game. For this comparison, the constant conditions would be the concentration of 20% and the same impact velocity of 3 mph. All of the strain data including ε_1, ε_2 and γ_{max} were collected as Table 4.1 and Table 4.3.

Table 4.3 Strain Value and Spatial Location Data of 20 Percent Gel Model with 3 mph Fore Head Impact.

	ε_1			ε_2			γ_{max}		
Rise Time(s)	0.004	0.004	0.003	0.005	0.005	0.004	0.003	0.004	0.004
Spatial Location	5	5	13	13	13	13	13	1	2
Strain Value	0.072	0.078	0.071	-0.067	-0.061	-0.06	0.089	0.087	0.082

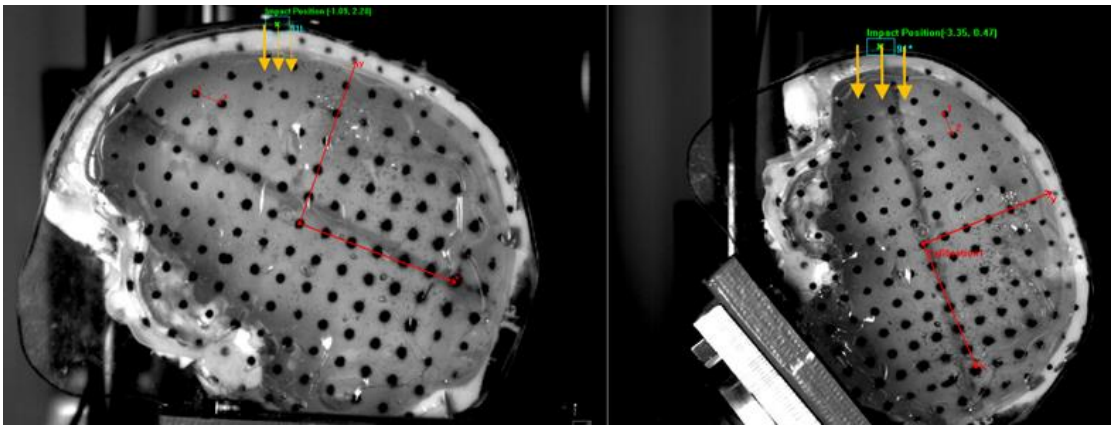

Figure 4.7 Different impact locations including crown head impact location and fore head impact location, yellow arrows indicated the specific impact location.

Comparing with the results from a crown impact, it was obtained that the mean of both strain value and rise time of fore head impact location were larger. In other words, the model with crown head impact location was deformed much more than the forehead impact location under the same conditions of the concentration of the gel (20%), and the same impact kinetic energy (Figure 4.8, Figure 4.9). There could be several assumptions for this result. First of all, it was assumed that the difference may came from the different skull deflections of different impact locations. The thickness of the skull in terms of the fore head impact location was thicker than the thickness of the crown head impact location, and the thicker part of the fore head skull would prevent much deformation of the inside gel from the impactor. The second area for potential differences is the boundary conditions applied to the skulls. In the forehead impact scenario, the neck allows stress relief to occur via movement. In the crown impact orientation, the neck cannot be compressed so nearly all the force of impact has to be absorbed by the skull and brain. This would lead to a greater degree of deformation and therefore strain.

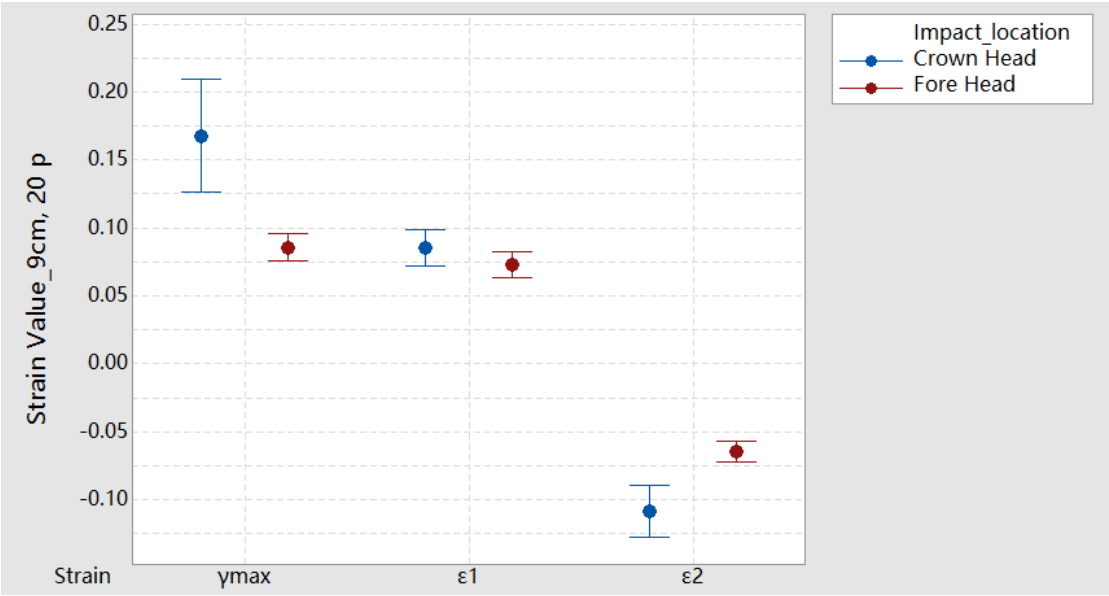

Figure 4.8 Strain value comparison between different impact locations (crown and front head) in terms of principal strain (ε_1 and ε_2) and maximum shear strain with 20 percent gel and 9cm of impact height, 95% CI for the mean.

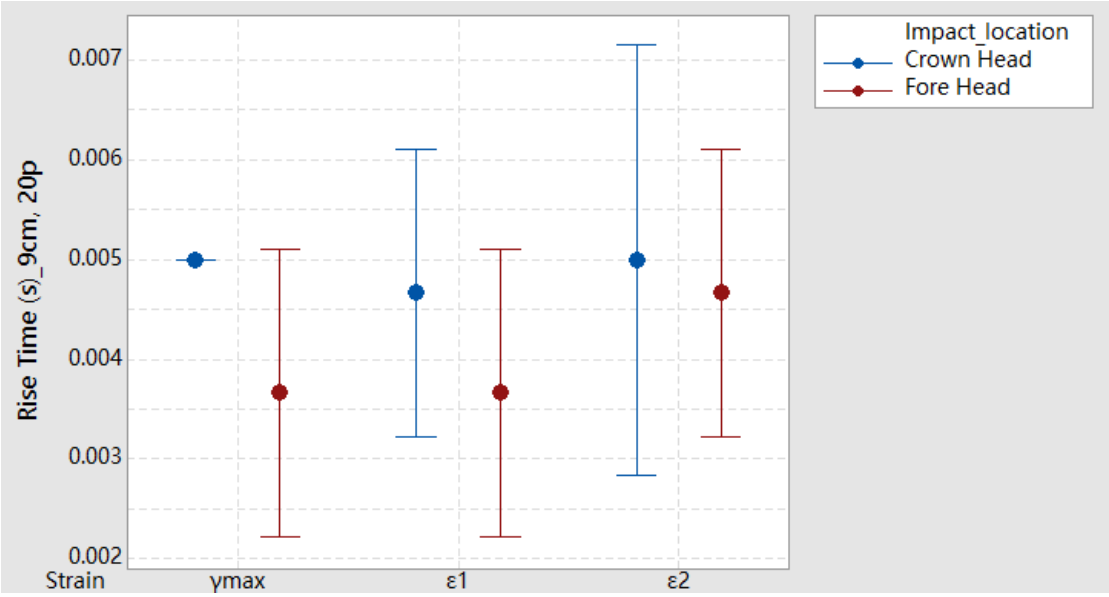

Figure 4.9 Rise time comparison between different impact locations (crown and front head) in terms of principal strain (ε_1 and ε_2) and maximum shear strain with 20 percent gel and 9cm height of impact height, 95% CI for the mean.

From the spatial location results (Figure 4.10), it was obtained that the maximum strains in terms of crown head occurred in 2nd and 3th quadrants, the maximum strains in terms of fore head occurred only in 2nd quadrant, which also had several assumptions. For the fore head impact location, in general, there should be some large deformation occurred at 3th quadrant area, because which was close to the impact location as much as the 2nd quadrant. However, the maximum strains did not located at 3th quadrant area, and two factors could lead to this phenomenon. First of all, the impact energy of the impactor giving to the model may be not large enough in terms of the impact height of 9cm, therefore the deformation in 3th quadrant was not transparent; Second, although both of the 2nd quadrant and 3th quadrant are close to the impact location, the structure of the skull near each of the two areas were not same, for example, the 3th quadrant was very close to the skull structure of the jaw, which was very possible can produce some boundary conditions for preventing the deformation of the inside gel. In addition the contour plot of all 72 squares' spatial results (Figure 4.11) indicated difference in terms of deformation pattern of different impact locations including crown head and fore head. Comparing with the pattern of crown head from top to bottom, the results shown the deformation pattern from 2nd quadrant to 1st quadrant in terms of the fore head because there were not so much deformation or strain values in the bottom area including 3rd and 4th quadrants, and it was also obtained that the plot of crown head held much more large and intensive strain area comparing with the fore head results, which was consistent with the results of the strain value.

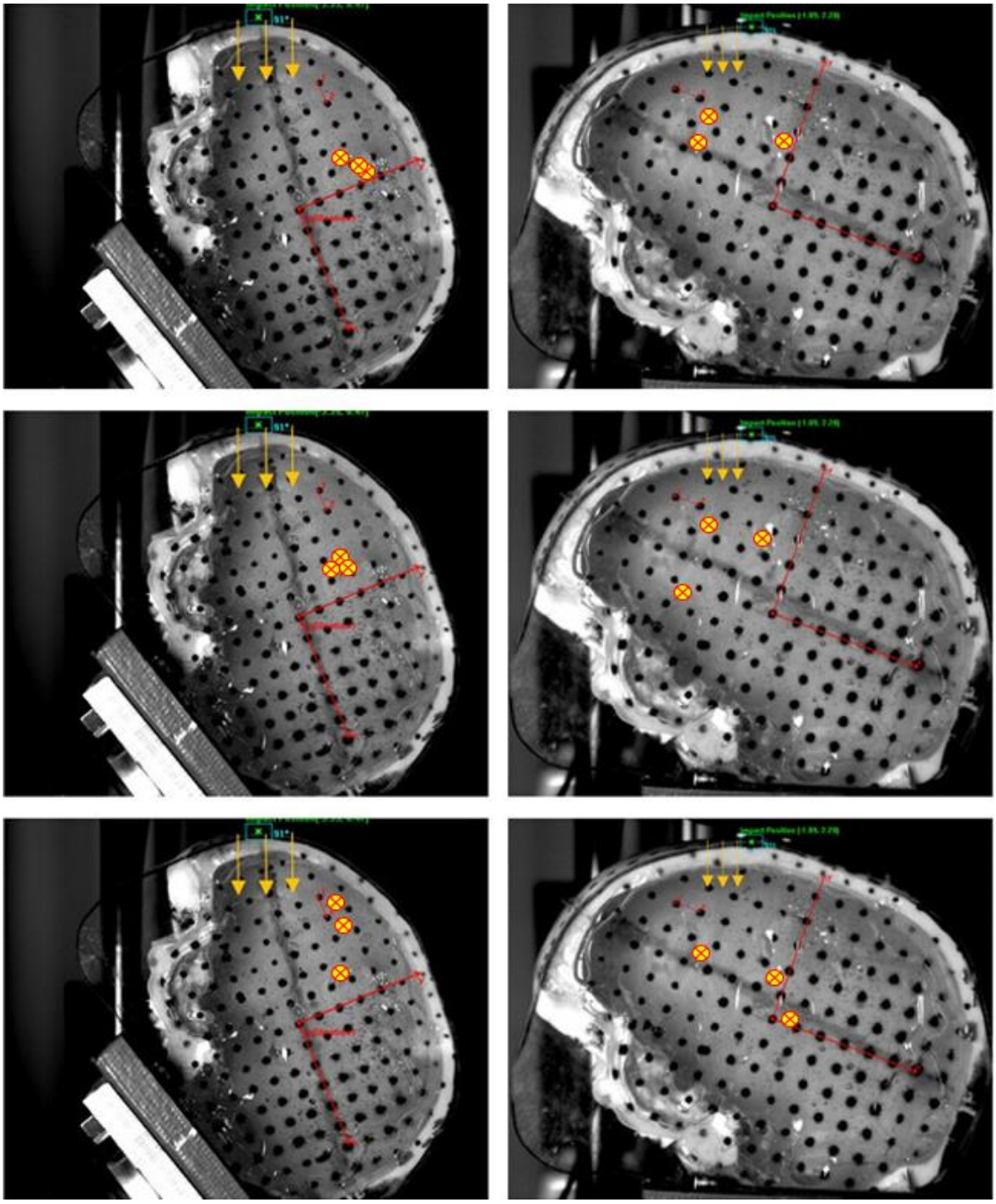

Figure 4.10 Spatial location comparison between different impact locations (crown position in first column, front head in the second column) in terms of principal strain (ε_1 and ε_2) and maximum shear strain from top to bottom with 20 percent gel and impact height of 9cm. Each yellow circle indicated the spatial location where maximum strain value appeared, and the impact locations were indicated by the yellow arrow.

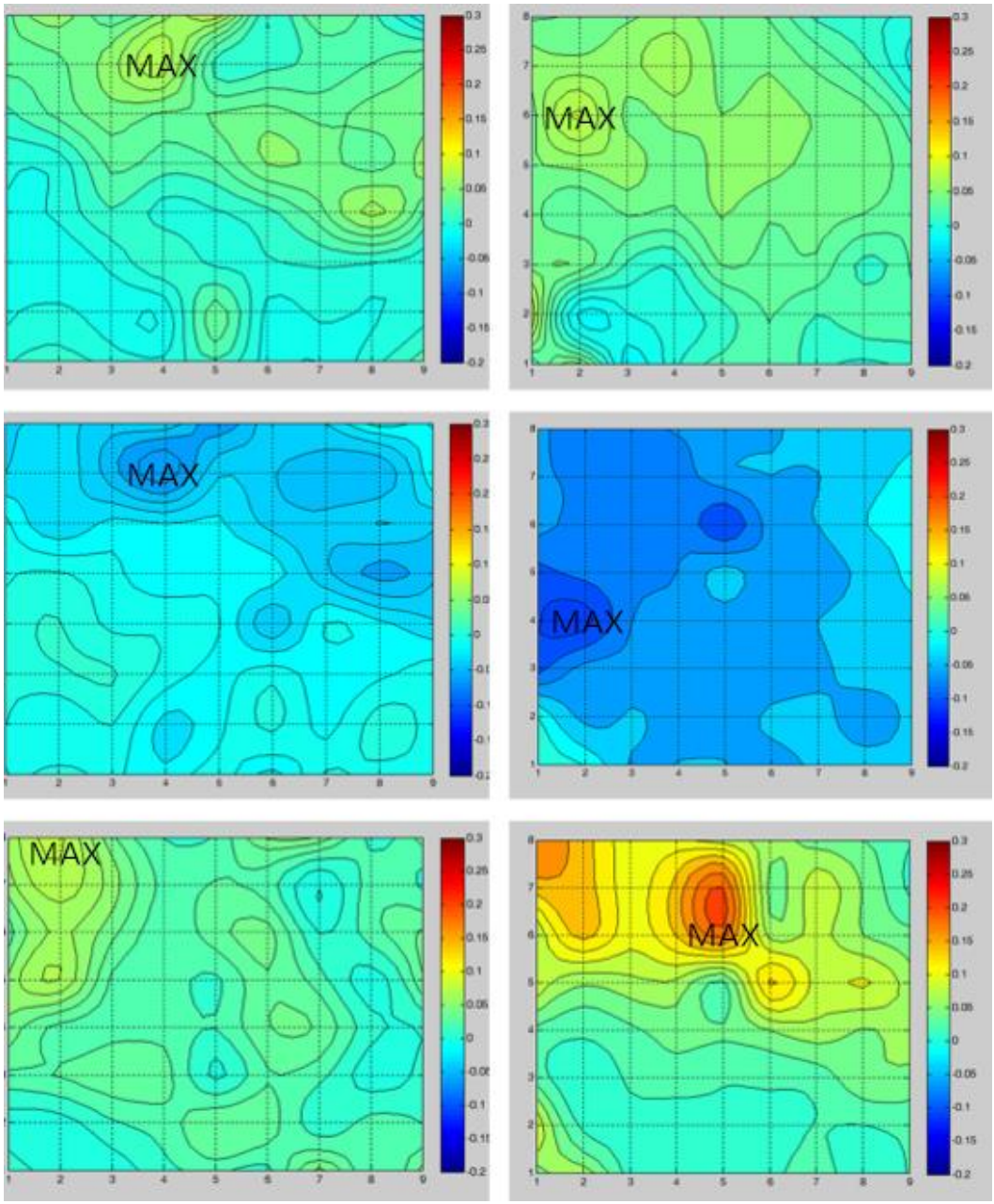

Figure 4.11 Comparison in terms of contour plotting all 72 squares between different impact locations (crown position in first column, front head in the second column) in terms of principal strain (ε_1 and ε_2) and maximum shear strain from top to bottom with 20 percent gel and impact height of 9cm.

4.3 Comparison Results with Different Gel Concentrations

The final variable used for comparison was the concentration of the gel. In this study, 10% gel and 20% gel were used for making the two head models, one of the reasons was that 10 percent gel could be much more similar to human brain in terms of the physical properties such as stiffness, which would be much more representative. For this comparison, the constant conditions would be the same impact location of fore head and impact height of 9cm. All of the strain data including $\varepsilon_1, \varepsilon_2$ and γ_{max} were collected as Table 4.3 and Table 4.5.

Table 4.4 Strain Value and Spatial Location Data of 10 Percent Gel Model with 3 mph Fore Head Impact.

	ε_1			ε_2			γ_{max}		
Rise Time(s)	0.006	0.006	0.009	0.009	0.009	0.006	0.008	0.008	0.006
Spatial Location	10	10	1	20	29	3	47	10	3
Strain Value	0.110	0.109	0.112	-0.112	-0.081	-0.138	0.146	0.177	0.124

Comparing with the results of 20 percent gel (Figure 4.12, Figure 4.13), the mean of the strain value and rise time of 10 percent gel were larger, which means that the model gel with 10 percent concentration was much more easily to be deformed, this result was consistent with the observation of the video coming from the high speed video camera system, which shown much more dispersion in terms of 10 percent gel on the surface of the markers during the impact time interval.

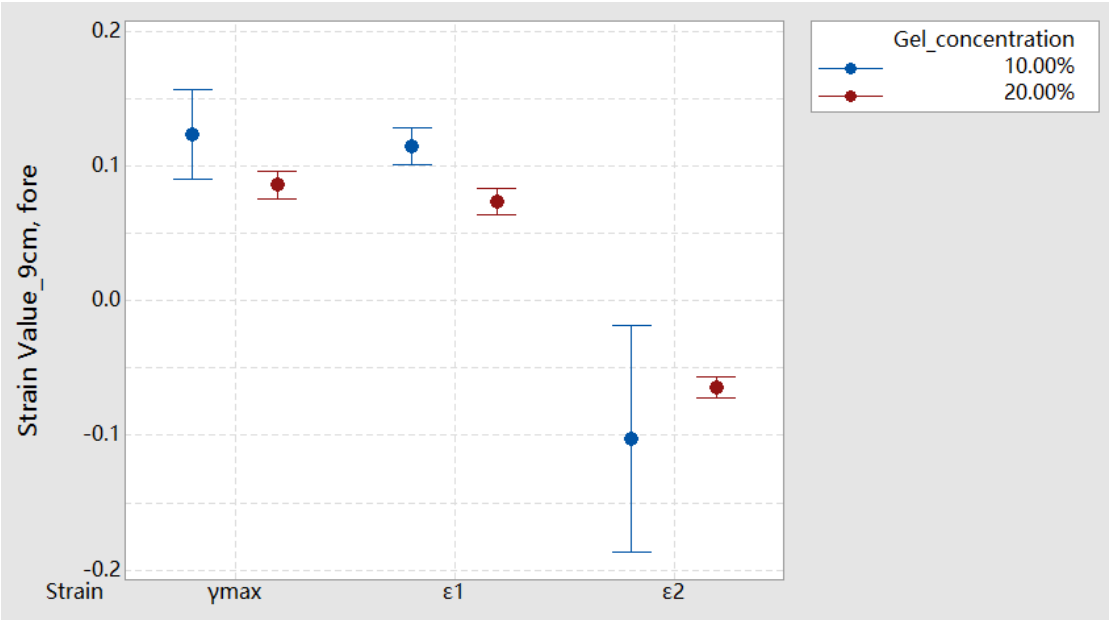

Figure 4.12 Strain value comparison between different gel concentration (20 percent and 10 percent) in terms of principal strain (ε_1 and ε_2) and maximum shear strain with impact height of 9cm and impact position of front head, 95% CI for the mean.

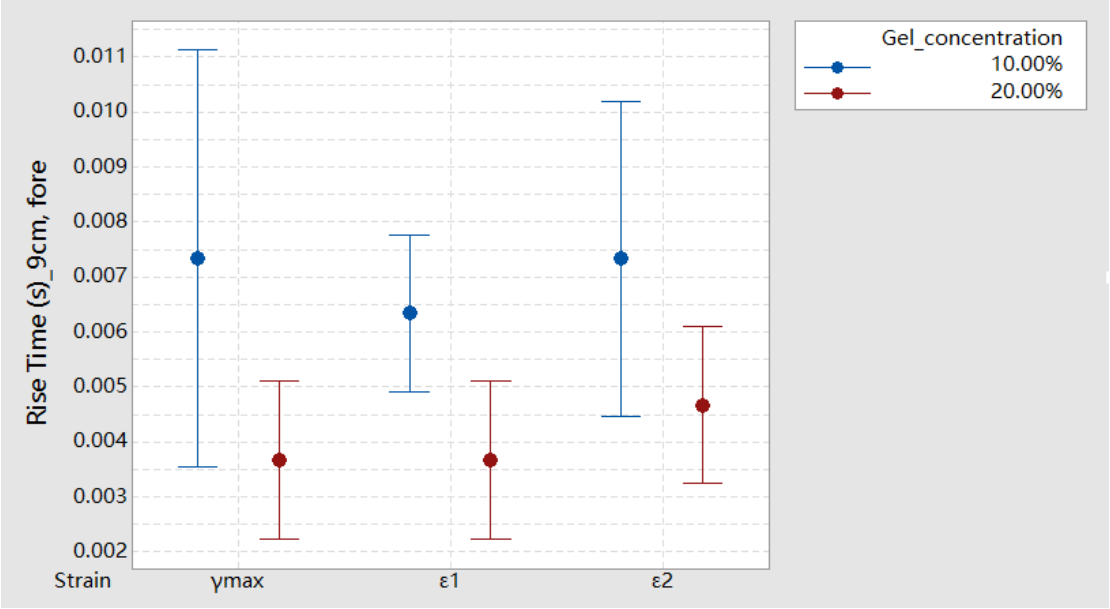

Figure 4.13 Rise time comparison between different gel concentration (20 percent and 10 percent) in terms of principal strain (ε_1 and ε_2) and maximum shear strain with impact height of 9cm and impact position of front head, 95% CI for the mean.

When it came to the spatial results (Figure 4.14), the locations of the maximum strain of 10 percent gel was more scattered than the locations of 20 percent gel (Table 4.5). This spatial result was really similar to the result with a higher impact height which was 25cm in this experiment and also occupied 2 quadrants. From the comparison of the contour plots (Figure 4.15), larger and more intense deformed areas from 2nd quadrant to 3rd quadrant were obtained including all of the 3 kinds of strain calculated in terms of the plots of 10 percent gel comparing with 20 percent gel. Different from the deformation pattern of the 20 percent gel, which was indicated by the right column of the contour plot showing horizontal pattern from left to right, the pattern of the 10 percent gel was not very clear because which actually spread nearly the whole 72 squares, which indicated that there would be still large deformation using 10 percent gel even if the impact energy the impactor transduced to the model was relatively small with impact height of 9cm, in other words, the concentration of the gel used for creating the head model also played a key role in the contribution for the study of deformation pattern with injury head.

Table 4.5 Mean Distance Between Two Spatial Locations of Maximum Strain Value of Different Concentration of Gels.

	ε_1(inch)	ε_2(inch)	γ_{max}(inch)
10% gel	0.25	0.75	1.32
20% gel	0.25	0	0.80

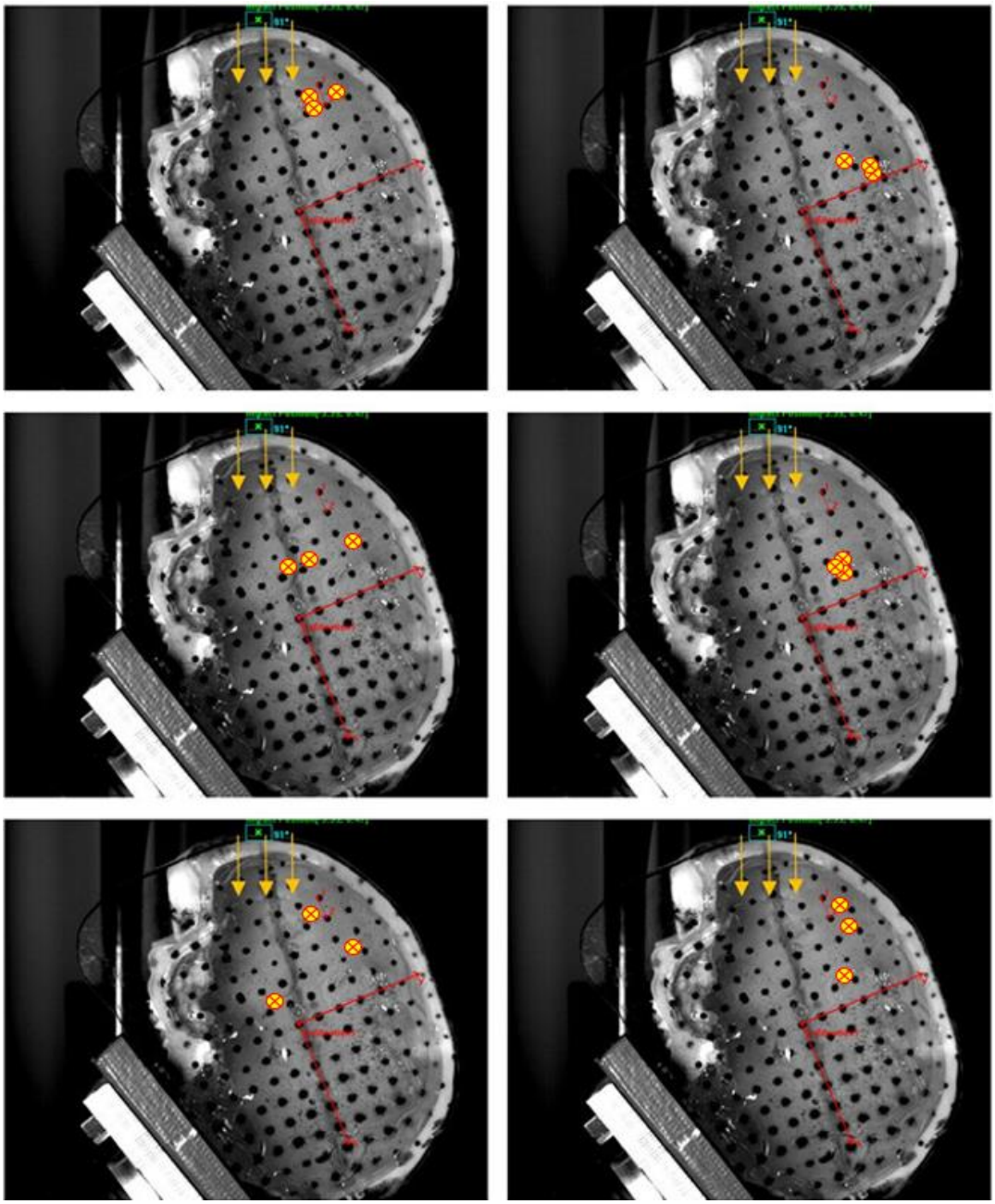

Figure 4.14 Spatial location comparison between different gel concentrations (10 percent in first column, 20 percent in second column) in terms of principal strain (ε_1 and ε_2) and maximum shear strain with impact velocity of 3 mph, impact position of front head. Each yellow circle indicated the spatial location where maximum strain value appeared, and the impact locations were indicated by the yellow arrow.

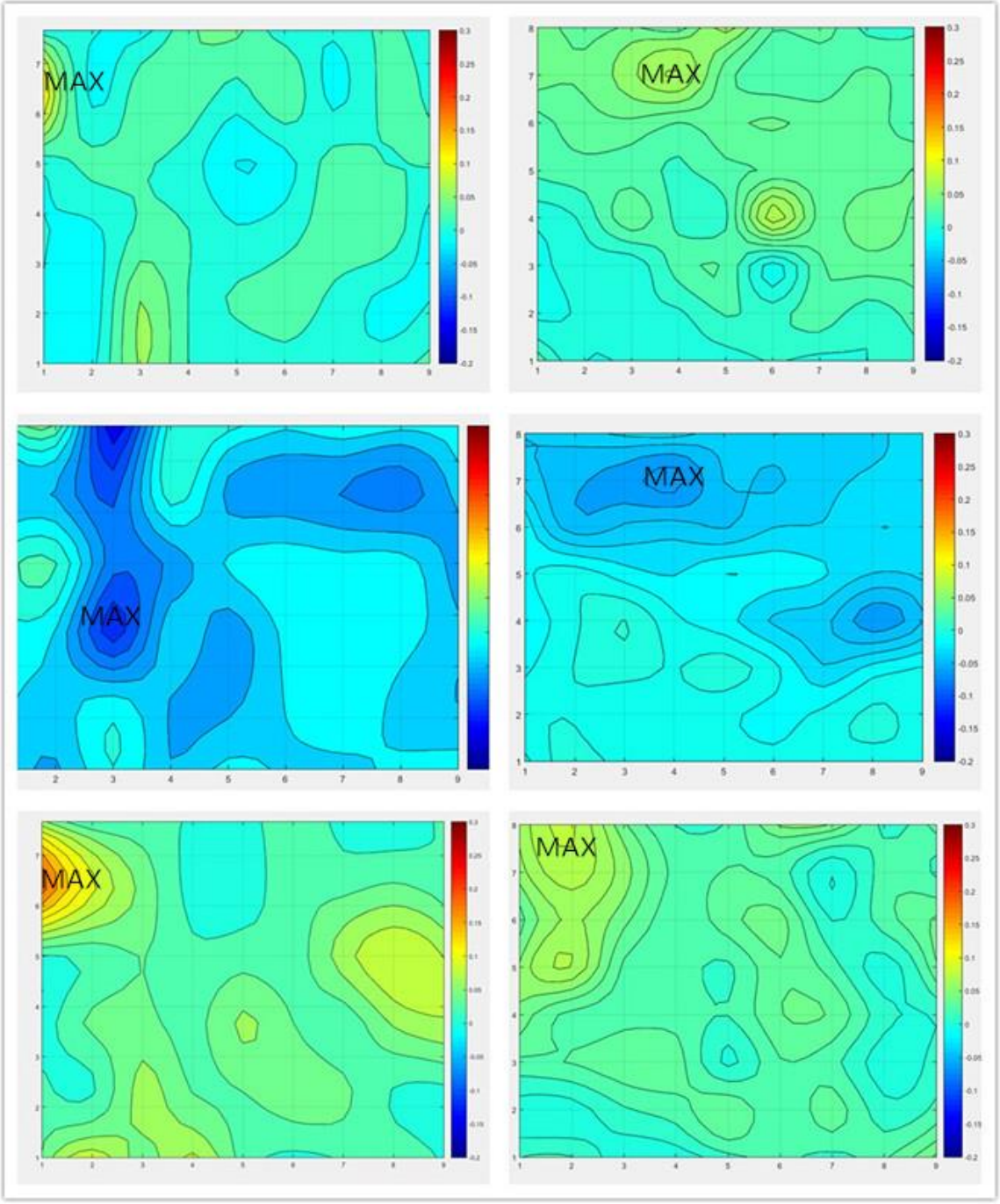

Figure 4.15 Comparison in terms of contour plotting all 72 squares between different gel concentration (10 percent in first column, 20 percent in second column) in terms of principal strain (ε_1 and ε_2) and maximum shear strain with impact height of 9cm, impact position of front head.

CHAPTER 5

CONCLUSION AND FUTURE WORK

In conclusion, the quantitative results show larger strain values within the variables of higher impact velocity, impact location of crown head and the concentration of 10% in terms of the gel used for creating the model; The spatial location results show different deformation patterns especially for the different deformation patterns of crown head and fore head.

There are some limitations that need to be improved in the future study. First of all, some material properties should be further examined including the impactor of the impact machine, and the different concentration of the gel. The properties of the impactor such as the stiffness should be examined because different impactors made of different materials will definitely have different effects on the head model. Additionally, it should be required to investigate the properties for the different concentration of gel in order to finding under what kind of concentration value the stiffness will be much more close to human brain tissue. The Young's Modulus of the gel can be calculated experimentally using either a rheometer or by finding the acoustic wave velocity of the gel. Density(ρ) is the ratio value of mass and volume, C can be calculated with the help of a shock tube, two different sensors can be placed before and after the material to measure the difference in the wave arrival time, and value of C can be represented by the ratio of inter sensor distance and difference in the arrival time.

$$C = \sqrt{\frac{E}{\rho}} \tag{5.1}$$

Second, during the impact test, not only the gel but also the skull would be deformed, it is necessary to track the movement or the displacement of the skull in future study in order to eliminating the effects of the skull deformation to the gel. Besides, when it comes to investigating different impact locations of crown head and fore head, the thickness of the skull should be investigated especially for the study of the spatial location. Third, higher impact velocity should be tested in the future, because in this study, the highest impact velocity is 5mile/hour, which is not very accurate for describing the impact velocity in reality where the impact velocity is much larger than 5mile/hour. Fourth, more complicated programming coding should be developed in order to mapping the whole area of the sagittal plane, and a new tracking tool should be considered because the tracking software used in this study can only track each marker manually, which really non efficiently increased the cycle time a lot. Fifth, in order to processing more statistic data and decrease the error, the repeat time of 3 in this experiment for each case should be increased.
This experiment will be helpful for measuring and presenting the deformation of brain with blunt injury, and make contribution for the future study of developing a comprehensive picture of the brain's behavior during acceleration.

REFERENCES

[1] http://www.cdc.gov/traumaticbraininjury/ (access on April 1, 2016).

[2] Holland, J.N. and A.T. Schmidt. (2015). Static and Dynamic Factors Promoting Resilience following Traumatic Brain Injury: A Brief Review. *Neural Plast*, 902802. doi.10.1155/2015/902802

[3] Delouche, A., et al. (2016). Diffusion MRI: Pitfalls, literature review and future directions of research in mild traumatic brain injury. *Eur J Radiol*, 85, 25-30.

[4] http://www.traumaticbraininjury.com/understanding-tbi/what-are-the-causes-of-tbi/ (access on April 1, 2016).

[5] http://www.biausa.org/mild-brain-injury.htm (access on April 1, 2016).

[6] Cairns, H. and H. Holbourn. (1943). Head Injuries in Motor-cyclists: with Special Reference to Crash Helmets. *Br Med J*, 1, 591-598.

[7] Pudenz, R.H. and C.H. Shelden. (1946). The lucite calvarium; a method for direct observation of the brain; cranial trauma and brain movement. *J Neurosurg*, 3, 487-505.

[8] Bayly, P.V., et al. (2006). In vivo imaging of rapid deformation and strain in an animal model of traumatic brain injury. *J Biomech*, 39, 1086-95.

[9] Wei, Liu, et al. (2004). HARP MRI Tagging for Direct Quantification of Lagrangian Strain in Rat Hearts After Myocardial Infarction. *J Biomech*, 126, 523-528.

[10] Gayzik, F.S., et al. (2011). Development of a full body CAD dataset for computational modeling: a multi-modality approach. *Ann Biomed Eng*, 39, 2568-83.

[11] Bayly, P.V., E.H. Clayton, and G.M. Genin. (2012). Quantitative imaging methods for the development and validation of brain biomechanics models. *Annu Rev Biomed Eng*, 14, 369-96.

[12] Bayly, P.V., et al. (2005). Deformation of the human brain induced by mild acceleration. *J Neurotrauma*, 22, 845-56.

[13] Feng, Y., et al. (2010). Relative brain displacement and deformation during constrained mild frontal head impact. J R Soc Interface, 7, 1677-88.

[14] Knutsen, A.K., et al. (2014). Improved measurement of brain deformation during mild head acceleration using a novel tagged MRI sequence. *J Biomech*, 47, 3475-81.

[15] Hardy, W. N., et al. (2001). Investigation of head injury mechanisms using neutral density technology and high-speed biplanar x-ray. *J Stapp car crash*, 45, 337-68.

[16] http://www.continuummechanics.org/cm/ (access on April 1, 2016).

[17] https://en.wikipedia.org/wiki/Finite_strain_theory (access on April 1, 2016).

[18] http://www.continuummechanics.org/cm/deformationgradient.html (access on April 1, 2016).

[19] Pfister, B. J., Weihs, T. P., Betenbaugh, M., & Bao, G. (2003). An in vitro uniaxial stretch model for axonal injury. *Ann Biomed Eng*, 31, 589-598.

[20] http://digitalcommons.unl.edu/dissertations/AAI3558421/ (access on April 1, 2016).

APPENDICES

SCRIPT FOR STRAIN TENSOR

```
%%Code to Find deformation gradient and principal strain of 90 markers
grid
%%in terms of 20 percent gel, impact location of fore head and impact
%%velocity of 3 mph by Chen Miao.

data = xlsread('20percent9cmforehead1.xlsx','A189:FZ488');
dummy = size(data);
quantity = (dummy(2)-2)/2;
%This loop will create a 300x2xquantity matrix, where each "page" is a
%separate point

count = 3;
for i = 1:quantity
    points(:,:,i)= data(:,count:count+1);
    count = count+2;
end
for j=1:79
    vectora(:,:,j) = points(:,:,j+1) - points(:,:,j);
    vectorb(:,:,j) = points(:,:,j+11) - points(:,:,j);
    undA(:,:,j) = [vectora(1,:,j)' vectorb(1,:,j)'];
    invundA(:,:,j) = inv(undA(:,:,j));

end
for j=1:79
     for frame = 1:300
       Fa(:,:,j,frame)              =              [vectora(frame,:,j)'
vectorb(frame,:,j)']*invundA(:,:,j);
       Ea(:,:,j,frame)                                                  =
((Fa(:,:,j,frame)'*Fa(:,:,j,frame))-eye(2))/2;
     end
end
% Script for creating deformation gradient(F) and Lagrangian strain
% tensor(E)


test = zeros(300,79);
for j =1:79,
for k = 1:201,
```

```
    testfa_xx(k,j) = Fa(1,1,j,k);
    testfa_yy(k,j) = Fa(2,2,j,k);
    testfa_xy1(k,j) = Fa(1,2,j,k);
    testfa_xy2(k,j) = Fa(2,1,j,k);
end
end
for j =1:79,
for k = 1:300,
    testEa_xx(k,j) = Ea(1,1,j,k);
%     testfc(k,j) = Fc(1,1,j,k);
    testEa_yy(k,j) = Ea(2,2,j,k);
    testEa_xy1(k,j) = Ea(1,2,j,k);
    testEa_xy2(k,j) = Ea(2,1,j,k);
end
end
for square = 1:79
    for t=1:length(testEa_xx)
       norm_p_strain_1(t,square) = (testEa_xx(t,square) +
testEa_yy(t,square))/2+sqrt(((testEa_xx(t,square) -
testEa_yy(t,square))/2)^2 + (testEa_xy1(t,square)/2)^2);
       norm_p_strain_2(t,square) = (testEa_xx(t,square) +
testEa_yy(t,square))/2-sqrt(((testEa_xx(t,square) -
testEa_yy(t,square))/2)^2 + (testEa_xy1(t,square)/2)^2);
       shear_p_strain(t,square) = 2*sqrt(((testEa_xx(t,square) -
testEa_yy(t,square))/2)^2 + (testEa_xy1(t,square)/2)^2);

    end
end
% Script For creating principal strain and maximum shear strain.

norm_p_strain_11=norm_p_strain_1;
norm_p_strain_11(:,10)=[];
norm_p_strain_11(:,20)=[];
norm_p_strain_11(:,30)=[];
norm_p_strain_11(:,40)=[];
norm_p_strain_11(:,50)=[];


norm_p_strain_22=norm_p_strain_2;
norm_p_strain_22(:,10)=[];
norm_p_strain_22(:,20)=[];
norm_p_strain_22(:,30)=[];
norm_p_strain_22(:,40)=[];
norm_p_strain_22(:,50)=[];
```

```
 shear_p_strain_33= shear_p_strain;
 shear_p_strain_33(:,10)=[];
 shear_p_strain_33(:,20)=[];
 shear_p_strain_33(:,30)=[];
 shear_p_strain_33(:,40)=[];
 shear_p_strain_33(:,50)=[];
%  Eliminate the outliers

subplot(2,2,1);
plot(norm_p_strain_11);
subplot(2,2,2)
plot(norm_p_strain_22);
subplot(2,2,3)
plot(shear_p_strain_33);

[max_1,frame_1] = max(norm_p_strain_11);
% Pick up the 72 max values for each square
[val_1,square_1] = max(max_1);
% Pick up the max value of 72 squares;
maxnorm_p_1 = [frame_1(square_1) square_1];
maxprin1=maxnorm_p_1;

[max_2,frame_2] = min(norm_p_strain_22);
% Pick up the 72 max values for each square
[val_2,square_2] = min(max_2);
% Pick up the max value of 72 squares;
maxnorm_p_2 = [frame_2(square_2) square_2];
maxprin2=maxnorm_p_2;

[max_3,frame_3] = max(shear_p_strain_33);
% Pick up the 72 max values for each square
[val_3,square_3] = max(max_3);
% Pick up the max value of 72 squares;
maxnorm_p_3 = [frame_3(square_3) square_3];
maxprin3=maxnorm_p_3;



max1=norm_p_strain_11(30,:)';
max2=norm_p_strain_22(33,:)';
max3=shear_p_strain_33(92,:)';
maxconp1 = zeros(8,9);
for frame =92
```

```
    i=1;
for row = 1:8
   maxconp1(row,1:9)=shear_p_strain_33(frame,i:i+8);
   i= i+9;
end
   maxconp = flipud(maxconp1);
   maxconq = interp2(interp2(maxconp,'cubic'),'cubic');
   figure
   colormap jet
   contourf(maxconq)
   set(gca,'xtick',1:4:33,'xticklabel',1:1:9);
   set(gca,'ytick',1:4:29,'yticklabel',1:1:8);
   grid on
   colorbar
   caxis([-0.2 0.3])
pause(.001)
end
% Finding maximum principal strain and maximum shear strain and plot
% spatial location of them using contour plot.
```